CHALMERS
UNIVERSITY OF TECHNOLOGY

Integration of fast charger stations

A technical investigation on grid connected high power converters and their filter solutions with focus on harmonic emissions and size reduction by utilising interleaved operation

Master's thesis in Electric Power Engineering

ADAM HULTIN
JOHAN WOLGERS

Department of Electrical Engineering, division of Electric Power Engineering
CHALMERS UNIVERSITY OF TECHNOLOGY
Gothenburg, Sweden 2017

Master's thesis 2017

Integration of fast charger stations

A technical investigation on grid connected high power converters and their filter solutions with a focus on harmonic emissions and size reduction by utilising interleaved operation

ADAM HULTIN
JOHAN WOLGERS

CHALMERS
UNIVERSITY OF TECHNOLOGY

Department of Electrical Engineering
Division of Electric Power Engineering
Chalmers University of Technology
Gothenburg, Sweden 2017

Integration of fast charger stations
A technical investigation on grid connected high power converters and their filter solutions with a focus on harmonic emissions and size reduction by utilising interleaved operation
Adam Hultin
Johan Wolgers

Supervisor: Gunilla Le Dous, Göteborg Energi Nät AB
Examiner: Torbjörn Thiringer, Department of Electrical Engineering

Master's Thesis 2017
Department of Electrical Engineering
Division of Electric Power Engineering
Chalmers University of Technology
SE-412 96 Gothenburg
Telephone +46 (0)31 772 1000

Cover: Illustration of a grid connected bus charger utilising a pantograph.
Illustration by Vincent Adler.

Typeset in LaTeX
Printed by Chalmers Reproservice
Gothenburg, Sweden 2017

Integration of fast charger stations
A technical investigation on high power converters and their filter solutions with a focus on harmonic emissions and size reduction by utilising interleaved operation

Adam Hultin
Johan Wolgers
Department of Electrical Engineering
Chalmers University of Technology

Abstract

In this paper, measurements are performed on an operating 300 kW bus charger station. A description of how the charger is constructed is given and the measurement results are presented. The efficiency of the charger was, at a 240 kW load level found to be around 95 %. The harmonic content is also presented for both current and voltage, and it was found to be within allowed levels specified in enforcing Swedish regulations, both in individual harmonic amplitudes and total harmonic distortion (THD). A simulation model has been constructed in PLECS®/Similunk® and the model was tweaked for the harmonic results to match those of the measurements.

Simulations of a 50 kW converter, switched at 25 kHz, has been performed in normal operation and interleaved operation for comparison of their emissions and the need of filtering. Simulations have shown that interleaved operation can fulfil valid standards and regulations of harmonics and opens for reduced filter size. The authors urges that a holistic view of the charger station is important to be able to reduce its total size. Further simulations with different real grid parameters have given support for that the grid location has a small or no impact on converter operation or risk of filter resonance.

Keywords: interleaved operation, filter, converter, bus charger, harmonic filtering, active rectification.

Acknowledgements

We would like to thank our examiner Torbjörn Thiringer, who has been supportive throughout the thesis work. A big thanks to Gunilla Le Dous and the others at Göteborg Energi Nät AB for a good time and the opportunity to take part in this research. Extra thanks to David Steen and Saeid Haghbin at Elkraftteknik, Chalmers, for supporting us with technical help and discussions. Also, thank you Vincent Adler for the beautiful cover page drawing.

Adam Hultin & Johan Wolgers, Gothenburg, June 2017

Glossary

LCL-filter Filter of third order, consisting of two inductors and a capacitor in a π structure. 2

PCC Point of common coupling is somewhere in the grid where a connections to other customers exist or can me made such as a bus-bar in a substation or a cable distribution cabinet.. 51

PLC A PLC is a very frequent used programmable computer in industry applications due to its reliability and simplicity.. xi

Acronyms

DSO Distribution System Operator. 18

EMC electromagnetic compatibility. 15
EMI electromagnetic interference. 1, 2, 15, 25, 35, 37, 54

FFT fast Fourier transform. 23

PCC point of common coupling. 15, 16, 18, 21, 59
PI proportional and intergrating. 36
PLC programmable logic computer . 20, *Glossary:* PLC
PLL phase locked loop. 39
PWM pulse width modulation. 8, 9

RMS root mean square. 26, 36

SiC silicon carbide. 39
SPWM sinusoidal pulse width modulation. 8, 9, 26
SVPWM space vector pulse width modulation. 8, 9, 39

THD total harmonic distortion. 6, 20, 48, 55, 66

Contents

1

Introduction

1.1 Background

In order not to jeopardise earth's climate, it is generally accepted that society needs to change its behaviour and adapt a more environmentally sustainable lifestyle [1]. It is well established that one of the ways this can be achieved is by reducing human caused CO_2 emissions.

One of the largest sources of CO_2 emissions is transportation, therefore a lot of effort has been focused on how to make transportation more sustainable [1]. One of the opportunities to reduce emissions of greenhouse gases may be to exchange vehicles with conventional combustion engines, to electric- or hybrid electric vehicles. By doing so, emissions may be reduced or at least confined to large production plants and more easily managed.

For electric vehicles to act as a serious alternative, charging them needs to be easy and more importantly, fast. As a result, the development of high power chargers is picking up speed. A number of more or less intricate solutions for rectification are available and all of them bring their own advantages and drawbacks. Often, a fast charger station takes up a lot of space, with bulky filter solutions required to reduce radiated electromagnetic interference (EMI) emissions to allowed levels. An effect of the large size is that the installation of charger stations in cities, with limited space, can be difficult. The converters can also be noisy when the switching frequency is within the hearing range.

It is for these reasons that this thesis studies and tries to quantify the weight and size of filter solutions for an existing active rectifier and investigates ways of reducing the size of such installations. With charger stations being less bulky and easier to install, people may be more inclined to install them, and the adaptation of electric vehicles can accelerate. Thus giving society a better chance at reduced CO_2 emissions.

1.2 Aim

The aim is to investigate an existing three-phase active rectifier's design and implementation, and verify that it fulfils applicable regulations and standards on current quality. To make a simulation model of a three-phase converter operating towards different grid conditions using grid filters, in order to map the interaction between grid and converter. To suggest ways that effectively reduces size of the converter installation whilst still fulfilling grid codes and regulation.

1.3 Problem definition

In order to reach the previously stated aim, the main problem is divided into smaller parts and corresponding problems are put into words as four questions. An initial insight about existing converters is desirable. How does an operating commercial charger behave in means of efficiency, emitted emissions and what filter solution is used?

From the results, how well does the investigated converter meet the available standards and regulations, and what regulations are applicable?

As mentioned, size is an important factor when installing chargers in urban environments. What parameter choices and design considerations can be made to reduce the size of the total installation?

Electronic equipment is susceptible to EMI from its surrounding. Does the location of the charger installation perhaps affect the amount of harmonic content that can be expected and does the grid robustness affect the operational stability of the converter?

1.4 Previous work

In [2], measurements have been performed on a 120 kW diode rectifier. The results showed high content of low order harmonics, thought to be partly because it did not operate at rated capacity. A way to reduce low order harmonics, is by using active rectification, pushing the most significant harmonics to the higher switching frequency, thus making them easier to filter.

A lot of research has been performed on active rectification and related control problems, over a long time [3]–[5]. The LCL-filter has grown in

popularity due to its low input impedance and has got a lot of attention in association with for example grid connected switched devices [6]–[9]. Even interleaved operation is a long time reoccurring concept [10], and research combining all of these concepts has already been covered extensively [11], [12].

What this thesis wants to highlight is the potential of reducing size, by using interleaved operation and increasing the switching frequency. Cancellation of the first switching frequency harmonics hopefully effectively reduces the size of the filter, and the entire rectifier. Active rectification and LCL-filters are very well covered subjects of research. This thesis tries to investigate an existing charging station. By creating a model based on the findings, the model can be scaled, filter solutions and modifications with the goal of reducing size can be proposed and tested. The robustness of the grid is also believed to play a part, and a smaller investigation of that is made through simulations.

1.5 Limitations

Throughout this thesis work, designed models are not realised in a physical prototype. Problems, such as unexpected effects of non ideal components are therefore overlooked. For a more thorough research, a prototype would have been desirable in order to give the results more substance.

Measurements are performed during real conditions on equipment connected to regular mains during normal operation. This causes difficulties to isolate external disturbances, that may affect the results.

Control is an important part of a converter, but the focus point of this thesis is to investigate harmonic content. Therefore, the control implemented follows simple, well established control procedures, not focusing on the stability of the system. Had there been an actual experimental implementation of a converter, a properly designed controller would have been of larger importance. All presented results are from steady state analysis.

2

Theory

This chapter is meant to be of help throughout the thesis, providing the necessary theory behind certain calculations and model choices. It starts off with the most fundamental concepts, fourier theory and the principles of rectification, and continues by diving deeper into filter design.

2.1 Fourier theory and harmonic content

As shown by Fourier, any periodic signal can be approximated by a sum of sinusoidal waves with different amplitudes and frequencies. Fourier analysis is a very powerful tool since it can quantify frequency content in a periodic signal. For electric power engineers it is especially useful since this tool can be used to express frequency content of a voltage and/or current. An example is illustrated in figure 2.1, where a periodic example signal can be represented as a sum of four pure sinusoidal waves.

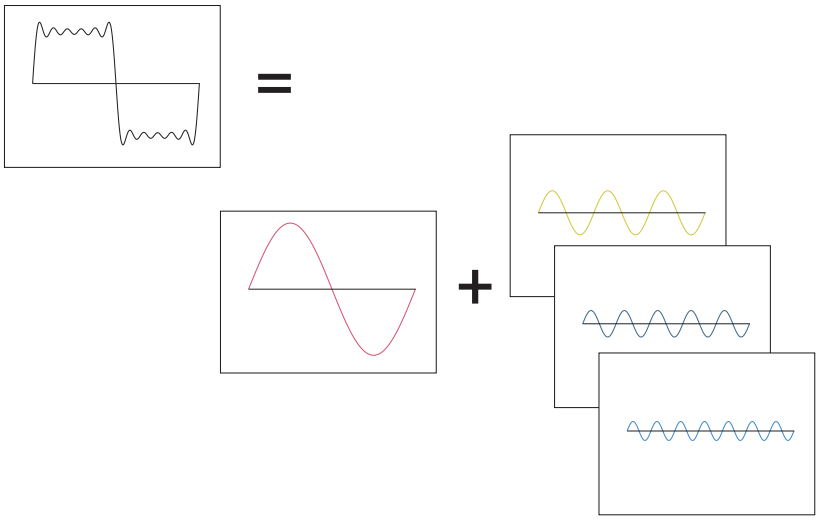

Figure 2.1: A periodic signal described by four periodic sinusoidal signals.

The mathematical representation of a general periodic signal $z(t)$ is

$$z(t) = \frac{a_0}{2} + \sum_{n=1}^{\infty} a_n \cos n\omega_g t + b_n \sin n\omega_g t \tag{2.1}$$

where ω_g is the fundamental frequency [13], and a_n and b_n are found as

$$a_n = \frac{2}{T}\int_0^T z(t) \cos n\omega_g t \; dt \qquad (n \geq 0) \tag{2.2}$$

$$b_n = \frac{2}{T}\int_0^T z(t) \sin n\omega_g t \; dt \qquad (n \geq 0) \tag{2.3}$$

where T is the timespan of the signal. A common way of presenting the harmonic content of a signal is through total harmonic distortion (THD) [14]. The THD is calculated as the ratio between the sum of the root mean squared harmonics and the fundamental as in

$$THD = \sum_{n=2}^{k} \frac{\sqrt{z_{(n)}^2}}{z_{(1)}} \tag{2.4}$$

where all up to the k'th harmonic, excluding interharmonics, are included. How many harmonics that are included differs. Swedish regulations define it to up to including the 40th harmonic and other standards define it to, for example up to the 50th [15], [16].

2.2 Principles of rectification

One of the simplest forms of 3-phase rectification is passive diode rectification. By utilising the diodes reverse voltage blocking ability, a DC voltage can be created. The circuit of a three phase rectifier is shown in figure 2.2. Each phase leg has two diodes attached to it, in opposite directions. The theoretical maximum voltage over the output capacitor C_{out} is the difference between the lowest and highest phase voltage.

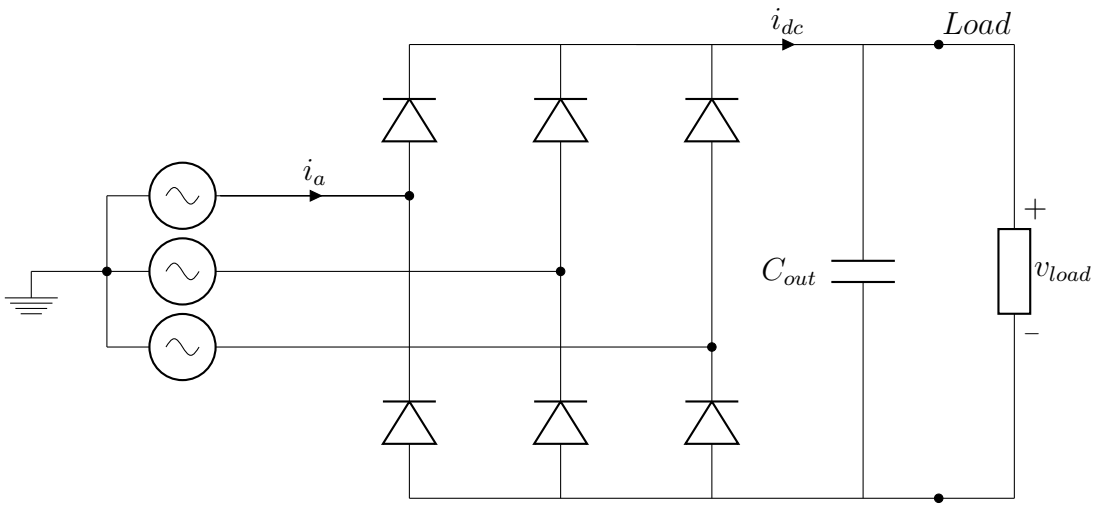

Figure 2.2: Circuit of a 3-phase diode rectifier

The output capacitor smoothens out the DC-voltage, which otherwise would consist of a ripple as shown in figure 2.3. The current i_a, drawn only when the line-to-line voltage, v_{dc}, is higher than the DC-link voltage, V_{DC}, is far from sinusoidal, thus it has a high harmonic content [17].

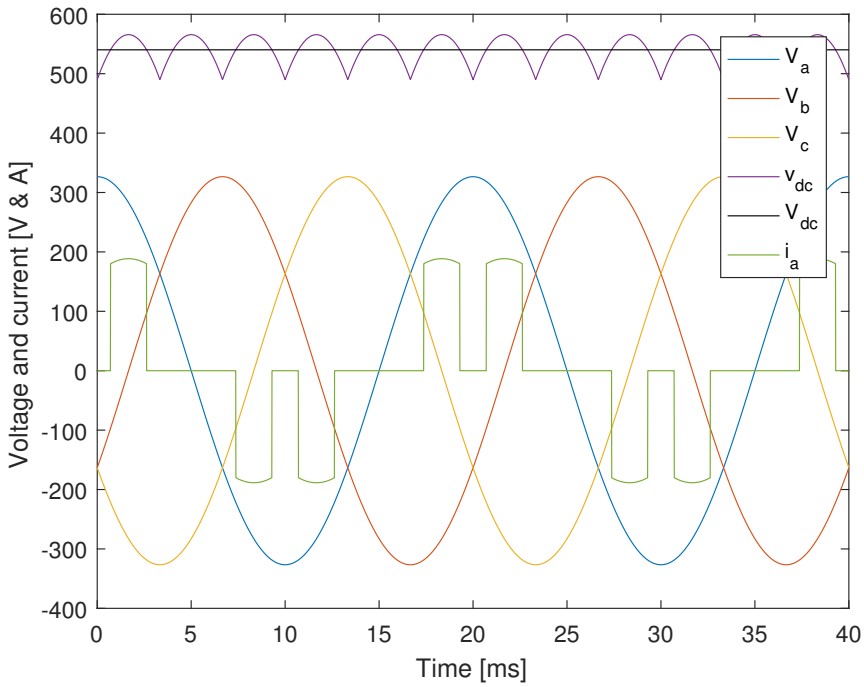

Figure 2.3: Diode rectifier voltage voltage and current wave-forms.

A conventional diode bridge rectifier is unidirectional due to the nature of the diode and can therefore only provide a positive current flow. It gives

no means of control-ability, since the diodes does not provide any way to control when to be turned on nor when to be turned off.

2.3 Signal modulation

In order to achieve controllability, the diodes can be exchanged to thyristors or transistors. With thyristors the turn on can be fired on specific timings to achieve increased controllability. This still yields low order harmonics and is still unidirectional. For full controllability and reduced low order harmonic content, transistors are needed.

The transisitors, connected with an anti-parallel diode, allows for full controllability of active and reactive power, sinusiodally drawn currents, four quadrant operation, and the ability to push harmonic content to higher frequencies. The working principle is that during short periods of time T_c, the voltage is applied to build an average voltage equal to the reference voltage. The first significant harmonic is now at the switching frequency f_{sw} [18].

There are different types of pulse width modulation (PWM) signal generation, for example sinusoidal pulse width modulation (SPWM) and space vector pulse width modulation (SVPWM), both of which are used in this thesis. In figure 2.4, the principle for SPWM is shown. The phase voltage references are compared with the common carrier signal, a triangle waveform with the frequency equal to that of the desired switching frequency. This comparison in turn generates on and off signals for the three phase legs.

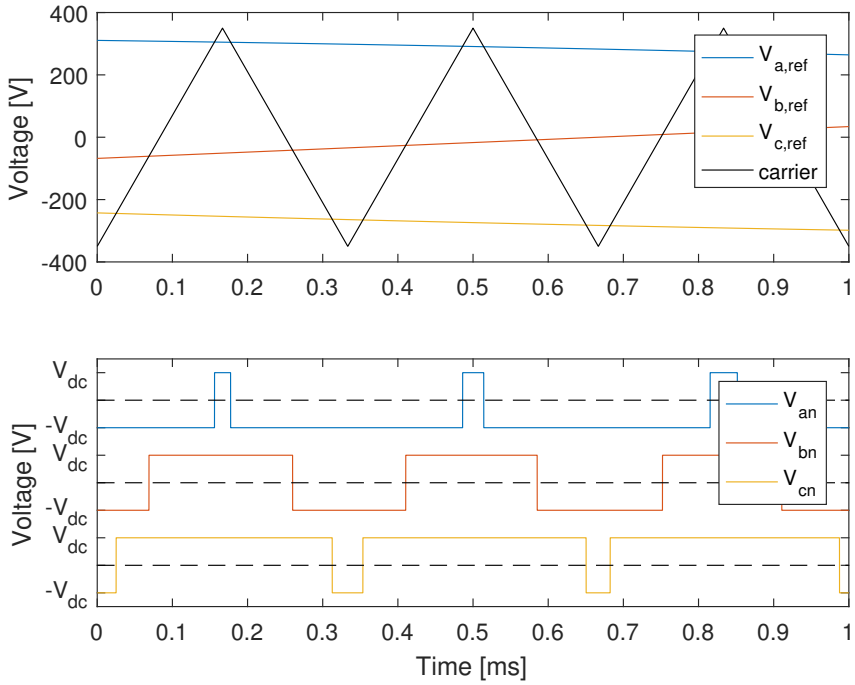

Figure 2.4: Carrier and reference comparison for generation of transistor gate signals.

As described, the SPWM method is built on direct comparison of carrier and reference. SVPWM on the other hand, can during one carrier period, create the target average voltage in many different ways. Each of them having its own advantage. Different types of PWM modulation techniques have different voltage harmonic spectras, and can be chosen based on the needs of the application.

2.4 Active rectification with PWM modulation

By changing the diodes to transistors, the phase legs can be actively turn on and turned off. This provides the ability to use PWM which generates a significantly more sinusoidal current. The most significant harmonic content of this technique is at the switching frequency. Pushing the significant harmonic higher makes it easier to filter with a low-pass filter. The DC link voltage can now be maintained at a level higher than the peak voltage of v_{dc} (as seen in figure 2.3), which is the maximum for diode rectification. This technique is called boost operation.

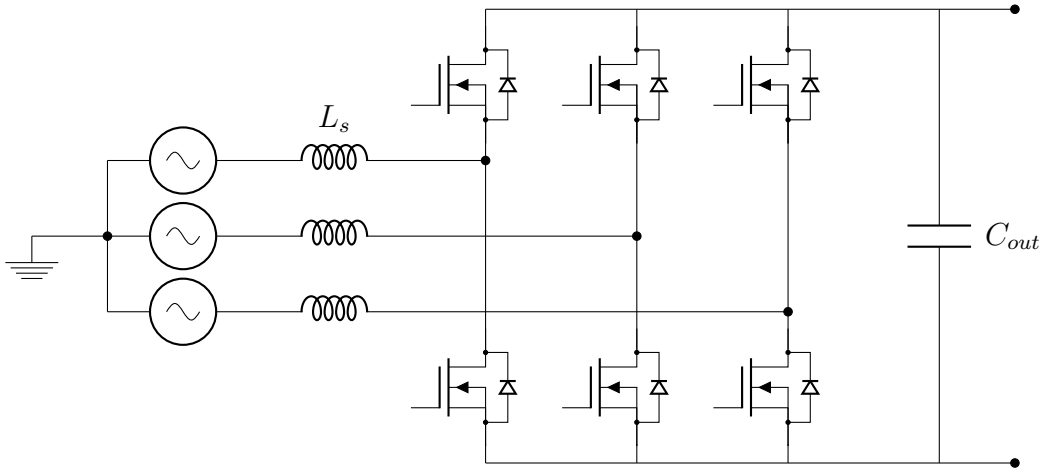

Figure 2.5: Circuit of active MOSFET rectifier

An example of drawn line current when using active rectification is shown if figure 2.6. The switching frequency used is in this case $f_{sw} = 3\ kHz$. Compared with the current drawn in the diode rectifier case, this is much more sinusoidal.

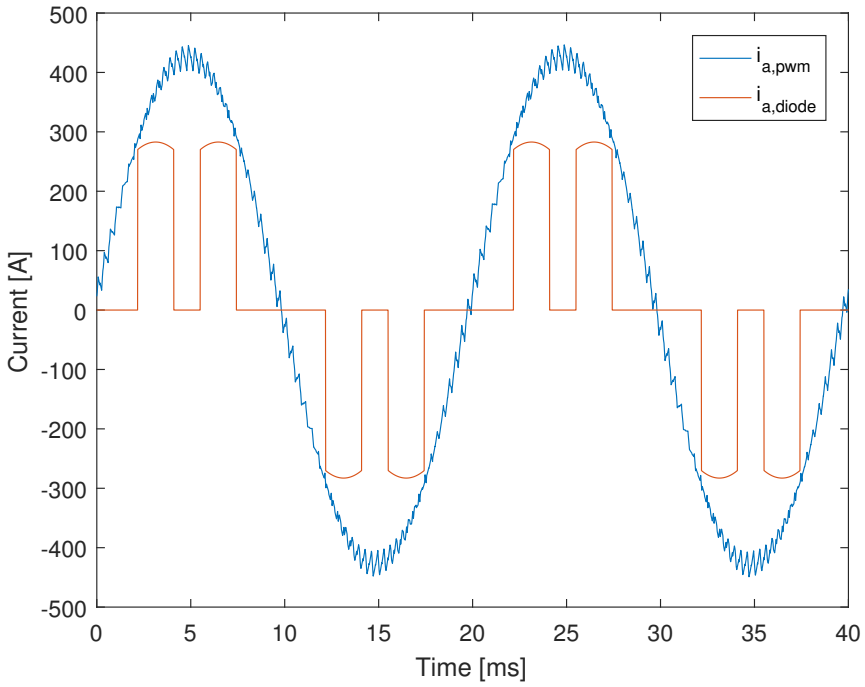

Figure 2.6: Drawn phase current when using active rectification compared to diode rectification.

2.5 Interleaved converter operation

Interleaved converter operation means to, when having two or more converters connected in parallel, phaseshift the carrier signal by $\frac{2\pi}{n}$, where n is the number of converters [19]. By doing so, the ripple at the switching frequency generated from each converter can effectively cancel out each other. This moves the most significant harmonics to two times the switching frequency, making it easier to filter. The paralleled converters can still share filter circuit, potentially reducing the size of the installation.

A problem that arises when operating interleaved is the phenomenon known as circulating current or cross current. It is the current that circulates between each converter stage, but it does not escape that mesh, and therefore does not affect the input harmonic spectra. This current does however yield losses in the semiconductors and it is desired to reduce the current as much as possible. A few different techniques to deal with this have been proposed, such as using certain SVPWM switching patterns to reduces the associated losses [10], and connecting series inductors in the circulating current path, or even using coupled inductors to further reduce the total size of the solution [20].

2.6 Harmonic filtering

The goal is to suppress influence of all frequencies higher than the fundamental. To easier describe a filters frequency behaviour the following filters are described in the frequency domain.

2.6.1 L-filter

A single inductor, in all its simplicity is traditionally a common way of filtering high frequency content as a series filter. The current stiff behavior of inductors is also both useful and necessary in the interface between the grid and converter to achieve boost operation. However this type of filter can only provide a theoretical attenuation of $-20\ dB/decade$ and the cut off frequency is directly controlled by the inductance value [21]. For high power applications, solely a single inductor as a filter risk of resulting in a more bulky and expensive filter solution than a more complex filter could have. Increasing the inductance value to lower the cut off frequency will not only result in increased physical size and cost but also increased losses and possibly decreased dynamic performance of the whole system [22].

2.6.2 High order filters

A particular type of higher order filters that is often used is the LCL filter. These filters are commonly used for grid connected switched-mode power converters [6], the fundamental circuit is presented in figure 2.7. A well designed LCL-filter can achieve advantages such as low impedance, high attenuation at reduced size and cost compared to a filter of first order [23].

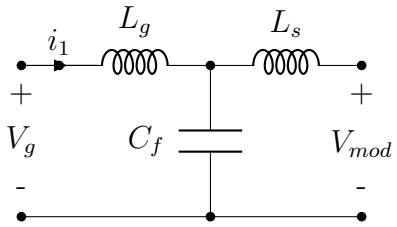

Figure 2.7: Circuit of LCL-filter.

The transfer function can, considering the case with no damper resistor [6], be determined as

$$H(s) = \frac{i_1(s)}{V_{mod}(s)} = \frac{1}{L_g L_s C_f s^3 + (L_g + L_s)s} \tag{2.5}$$

where s is the Laplace transform variable. With the addition of the damper resistor R_d, the transfer function can be rewritten as

$$H_d(s) = \frac{C_f R_d s + 1}{L_g L_s C_f s^3 + C_f R_d (L_g + L_s) s^2 + (L_g + L_s)s}. \tag{2.6}$$

The damped circuit is shown in figure 2.8.

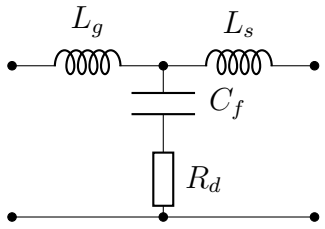

Figure 2.8: Simple LCL-filter circuit with damping resistor

A bode plot of the undamped and damped transfer functions for an LCL-filter is illustrated in figure 2.9. By adding the damping resistor the gain

peak at the resonance frequency has been reduced at the cost of some energy loss in the resistor and slightly less damping above the cut off frequency.

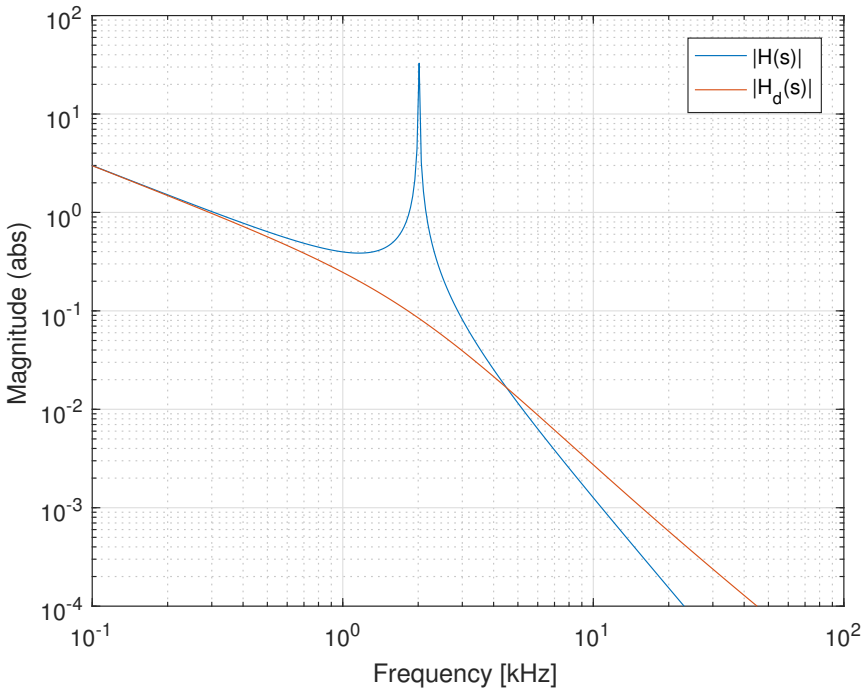

Figure 2.9: Bode diagram of an LCL-filter with and without damping resistor.

3

Measurement setup, grid model and harmonic limitations

This chapter contains information of how power quality is defined in this thesis and which components within the subject of power quality that is analysed in this report. The chapter also tries to state how electric power quality is measured. The thesis also tries to describe important properties of a converter in this size and how it can be related to the strength and robustness of the grid. Furthermore, in order to support the results of the simulations made in chapter 5, measurements on an existing 300 kW bus charger are performed as a part of this thesis. By doing so, the measurements are used as reference to verify that the simulated values are within close proximity of a real, already operating, fast charger. Furthermore, these measurements will also try to visualise the quality of the model.

3.1 Grid modeling

It is assumed that a converter of this size is fed through a public grid. As for many electronic components it is important to fulfil electromagnetic compatibility (EMC) conventions not to cause unintentional interference with other electric equipment. There are a lot of factors that can cause EMI, some examples are bad design or improper installations. EMC states the ability for equipment to operate as indented in an environment of electromagnetic disturbances and also not to disturb other equipment by broadcasting electromagnetic emissions. Switched power electric converters have a natural behaviour of drawing a current with a considerable amount of harmonics which can spread and cause harmonic voltage fluctuations in the point of common coupling (PCC) and therefore also might disturb other electric equipment.

The grid is chosen to be represented by a simple circuit, a Thévenin equiva-

lent. In figure 3.1, a single line diagram of a grid Thévenin equivalent representing a larger grid is presented. The grid is represented by an ideal voltage source and an impedance, $Z_k = R_k + jX_k$. The short circuit impedance Z_k which represents the impedance in the grid such as electrical lines, transformer impedance etc. From this scheme it is trivial to understand that a current with harmonic content drawn at the PCC will cause a voltage drop over Z_k and therefore create a harmonic content of the voltage in the same location.

The PCC is where the measurements are made. There definition of PCC can vary slightly depending on the source. The definition in this thesis is chosen according to [24] as *"The PCC is the point of metering of power supply from the utility to a customer (...) (and) The PCC is also the point where another consumer can be served from the same system..."*. In practice this can be interpreted to different locations in the grid such as a cable distribution cabinet, just before a customers meter depending or at the bus bar on the secondary side of the transformer, all depending on the specific conditions at each location. However, in this thesis measurements are performed close to the customer meter due to practical issues and simulations are performed for short circuit impedances at the closest cable distribution cabinet.

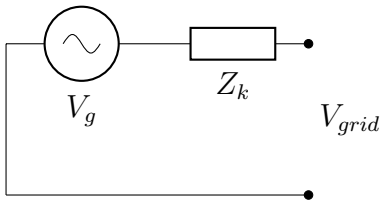

Figure 3.1: Thévenin equivalent

In co-operation with *Göteborg Energi Nät AB*, a few locations which could be candidates for installing bus charger stations in the future are selected and its locations is presented on the map of Hisingen in figure 3.2. In order to find a Z_k equivalent for the selected locations, theoretically calculated impedance, voltage and short circuit power values for the closest secondary substation are provided from the grid company. Together with the calculated impedance of the feeding cable to a cable distribution cabinet, these values are added together to represent the grid. The cable impedance, Z_c is calculated as

$$Z_c = \ell \left(R_c + j\omega L_c \right) \tag{3.1}$$

where ℓ is the length of the cable in m, R_c and L_c is the cable resistance and inductance per m. The resulting values of both short circuit impedance at the transformer and series impedance in low voltage cable is presented in table 3.1. They are used for simulations with the different filter solutions in chapter 5.

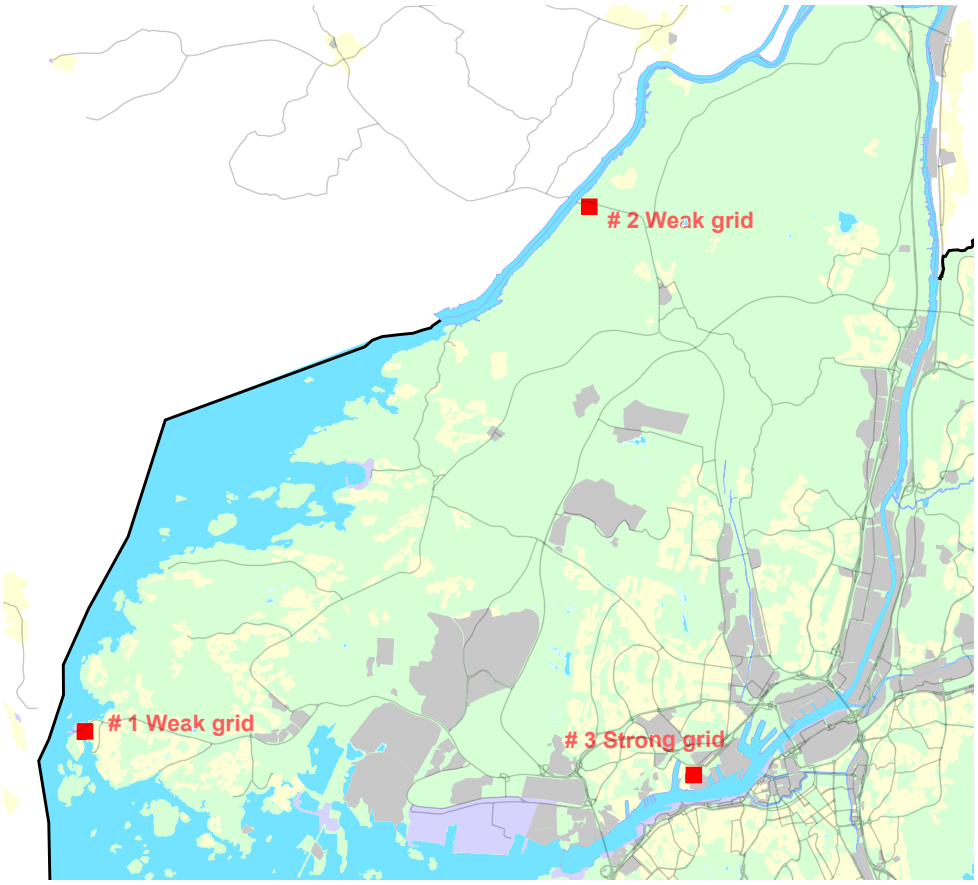

Figure 3.2: Example locations on Hisingen, Gothenburg used for simulations of grid influence.

Table 3.1: Short circuit parameters at different grid locations. All parameters are with respect to a main voltage of 400 V.

Location	R_k $[m\Omega]$	X_k $[m\Omega]$	L_k $[\mu H]$	**Distance*** $[m]$
#1 Weak grid	41.9	34.4	109	211
#2 Weak grid	35.1	38.8	124	220
#3 Strong grid	10.7	14.0	44	133

**Distance is approximated length of low voltage cable from transformer to converter.*

3.2 Harmonic content, recommendations and limits

There are a few international standards addressing harmonic content levels in an electric grid, for example IEEE Standard 519-1992, 519-2014 and

IEC Standard 61000-3-6 [25]. A majority of occurring standards was however, created at a time when switched converters were less common and is mainly addressing limits of lower order harmonics of the grid frequency. The IEEE 519-1992 is for example addressing limits up to the 35:th harmonic and IEEE 519-2014 up to the 50:th harmonic which would represent 1.750 kHz and 2.5 kHz respectively. The voltage limits according to the IEEE 519-2014 is presented in table 3.3. Compared to common high frequency switched converters operating at a switching frequency of typically some kHz these grid codes may not be applicable. Regulations or minimum standards are typically set up by authorities in each country or region. In Sweden for example, there are (at least) two documents addressing electric power quality in public electricity networks, the statute EIFS 2013:1 [26] and the standard SS-EN 50160 [15]. Ultimately it is up to each Distribution System Operator (DSO) (grid owner) to decide if they will stricter limits of harmonic content in the grid. Generally, the operator is responsible to keep the voltage harmonics within certain levels, whereas the customers allowed harmonic pollution is specified in current harmonics [27]. Current harmonics according to [15] is presented in table 3.2. The standards are usually describing a tolerance for a total amount of harmonic distortion in a PCC which means that the standard describes the sum of harmonic contribution from all customers and it is up to the grid owner to handle how the space for harmonic content is shared between different customers.

Table 3.2: Example of limitations of harmonic content according to Swedish national regulations EIFS 2013:1 [26].

Uneven harmonics				**Even harmonics**	
Non multiples of 3		Multiples of 3			
Harmonic [n]	Limit %	Harmonic [n]	Limit %	Harmonic [n]	Limit %
5	6.0	3	5.0	2	2.0
7	5.0	9	1.5	4	1.0
11	3.5	15	0.5	6-24	0.5
13	3.0	21	0.5		
17	2.0				
19	1.5				
23	1.5				
25	1.5				

Table 3.3: Voltage harmonics limits specified in IEEE Standard 519-2014 [16]. Less than 1 kV is the voltage level relevant in this thesis.

Voltage V at PCC $[kV]$	**Individual harmonics** [%]	**THD** [%]
V$\leq$ 1	5.00	8.00
1 <V$\leq$ 69	3.00	5.00
69 <V$\leq$ 161	1.50	2.50
161 <V	1.00	1.50

Seen from a grid-owner perspective a low amount of harmonic content is desirable. The susceptibility of harmonics for connected equipment varies depending on type of equipment along a floating scale. Some equipment require a more or less perfect sinusoidal voltage to operate properly (for example some measurement- or communication-devices); while resistive devices for heating can on the other hand be placed in the opposite side of the same scale as it has low susceptibility for harmonics, the energy in the harmonic content will then be utilised as heat [28]. The presence of harmonic content can cause severe problems for a variety of other equipment, for example:

- Increased currents in the system such as harmonic caused high neutral current when the sinusoidal currents fail to level out and can cause overload in transformers, capacitors, distribution systems etc.
- Increased losses and heat dissipation in equipment such as motors or transformers due to undesirable eddy currents causing core losses.
- Pulsating torque in motors.
- Acoustic problems such as interference with telephone lines or causing mechanical resonance caused by magnetic fields.
- Disturbances in electronic equipment such as computers, measurement equipment, large motor controllers etc. due to quality problems with feeding power [28].

There are also standards defining detailed specifications on how to quantify and measure harmonic content. Such standards often also includes statistical models of how to interpret the results such as *"IEEE recommended practice and requirements for harmonic control in electric power systems"* [16]. Some measurements require long term measurements (typically several weeks) and others are defining short term occurring harmonics down to fractions of seconds. However, measurements done in this thesis is only done over a short time span, more precisely during one day.

3.3 Power quality measurements at Lindholmen, bus line 55 charger

The new bus line, 55 has 10 buses operating daily, out of which 3 are driven solely on electricity whereas the others are plug-in hybrids. The line is operating at daily service between Chalmers university's two campus in Gothenburg since year 2015. End stations are at Teknikgatan, Lindholmen and Sven Hultins plats, Johanneberg where fast chargers are located [29]. The chargers are equipped with a standardised OPPCharge interface [30]. This interface defines both standards for communication between the charging vehicle and the charger as well as how the electrical connection is performed. The OPPCharge interface has current collectors mounted on the charger station instead of the vehicle (which is normal on most trains, trams and trolleybuses). The charger is designed for a maximum of 300 kW charging power but is with the current busses operating at a lower power. The charger uses active rectification with two parallel IGBT stages operating at a switching frequency of 3 kHz. The busses charge at a typical maximum power of $\sim$ 240 kW, depending on type of bus. In figure 3.3 a principle circuit for the grid connected charger is shown. The converter has two parallel AC/DC stages and each of them are preceded by an internal choke reactor (L_1 and L_2) of 600 μH. Prior to the converter there is a 400 : 230 V DY-transformer operating both as a filter and providing galvanic isolation. There are also two 3-phase capacitors connected on the converter input, is it suspected that they are connected between the transformer and the choke reactors and the setup will in that case function as an LCL-filter. Next to the grid there is a filter with unknown parameters. The whole setup is connected to the substation with two parallel 240 mm^2 Al cables. According to technical specifications for the converter its THD is stated to be less than 8 % in accordance with IEC 61000-2-2.

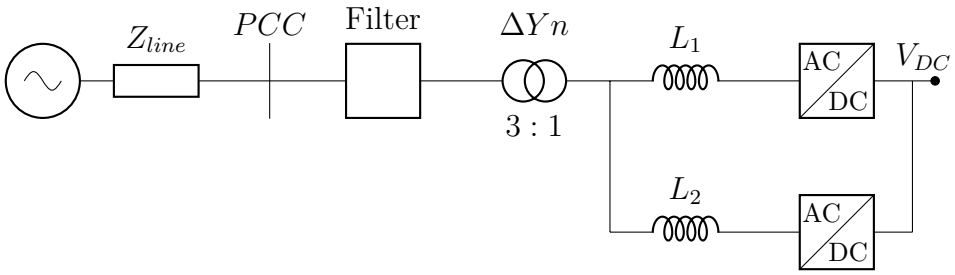

Figure 3.3: Principle diagram of Siemens charger

The installation on Lindholmen consists of two parts where the first one is in the indoor bus stop containing more or less what the travellers can see such as pantograph, positioning control etc. The second part is located in a garage in the basement of the connecting building and contains PLC au-

tomation, energy metering, the converter and the comparatively large transformer. The full installation in the garage includes (beyond the converter), ventilation fans, door control, energy metering, fuse box etc. The allocated space is approximately the size of two regular parking spaces where most of the space is service space. If you only count effective space for the converter and its filters it is a lot less. The converter cabinet also holds components responsible for pantograph control, bus communication etc. A summary of weight and size is presented in table 3.4. It is obvious from this description that there is a large difference between the total allocated space and the necessary effective space and accordingly there should be opportunities for a significant space saving.

Table 3.4: Approximated size and weight of Siemens installation.

Component	**Size** $[m^3]$	**Weight** $[kg]$
Transformer	1.25	1 290
Cabinet	3.36	983
- *Inductors**	0.3	360
- *Capacitors**	0.003	4
Total	4.61	2 273

**The inductors and capacitors are placed inside the cabinet and the weight of them is also included in the one listed for the cabinet.*

3.3.1 Measurement setup at Lindholmen

By today there is only one electrified bus line in Gothenburg. The previously mentioned charging station at Lindholmen is chosen as a subject for measurements. These measurements aim to investigate the magnitude and frequencies of harmonic emissions from a typical high power AC/DC converter in operation. Both of the charger stations are supplied through a relatively strong grid. Due to practical reasons the charger on Lindholmen is selected as a subject for measurements.

Voltages and currents are measured at the grid connection (PCC in figure 3.3) and on the secondary side of the filter (right side of filter in the same figure) during both high- and low power charging cycles (electric bus respectively hybrid bus). No significant difference was noticed and the PCC values are selected for calculations) Both charging cycles are however of lower power than the rated power for the converter. Since disconnection of conductors was not possible, openable current clamps are selected. CWT3s from Power electric Measurements Ltd. are chosen for measuring AC currents which is of Rogowski type, one of the used current meters is displayed in figure 3.5b. One of the benefits with these current probes is low noise levels and ability to encircle both of the thick parallel conductors at once.

Rogowski coils are not able to detect DC currents, therefore a TA019 current probe from Picotech which is of hall effect type, illustrated in figure 3.5a, is selected and used for DC current measurements. Voltages are measured with Testec TT-SI 9010 differiental probes illustrated in figure 3.4a. An 8 channel computer oscilloscope PicoScope 4824 with 12 bits resolution is used for sampling the currents and voltages. The Picoscope is illustrated in figure 3.4b.

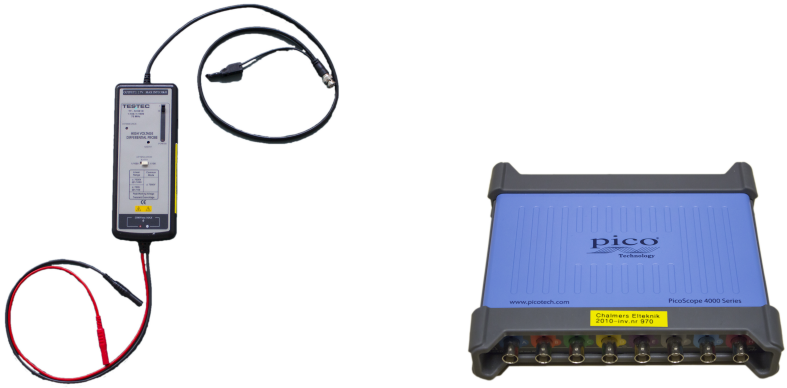

(a) Testec TT-SE 9010 **(b)** Picoscope 4824

Figure 3.4: Differential probe and computer oscilloscope.

(a) Picotech TA019 **(b)** Rogowski coil

Figure 3.5: DC current probe and Rogowski type AC current probe.

3.4 Processing measurement results

Measured voltages and currents from the measurements in 3.3.1 are sampled with uniform time steps and can easily be analysed in MATLAB. Shorter time intervals are extracted from the measurements when the converter is operating in steady state. These measurements are used to calculate instantaneous, as well as mean, power P_{in} and P_{out} and efficiency η. Frequency

content is also calculated with the fast Fourier transform (FFT) for achieving an observable energy spectrum.

3.4.1 Frequency content

The measurements are sampled at even distributed time intervals and with many sample points but the sample intervals is not necessary start and end with full fundamental sinusoidal periods. The window function *flat top window* that is common in spectral analyzers, is applied to improve amplitude representation at the cost of frequency resolution and high noise bandwidth.

4

Filter design

Filters are an important and necessary part of a converter to limit its EMI. The design of filters is a frequently overlooked subject and commonly paid too little attention to. All too often, the filter is considered first after a design process, such as when a prototype failed to work or a model turned out not to fulfill existing standards. It is not obviously intuitive that a filter for a power electric system actually is a part of the converter; in fact, the filter influences both output impedance as well as control feedback loop (and therefore also transfer function) and should therefore be considered to be a part of the converter instead of a circuit of its own [23].

The design process of a filter includes many considerations and difficulties and can therefore be difficult to describe in a general manner. In this thesis an LCL-filter is designed for a 50 kW charger switched at 25 kHz. This chapter aims to explain the design methodology used for retrieving the filter parameters, both in normal operation and interleaved operation.

4.1 Estimation of required attenuation

In order to minimise the size of a filter, the restraints set by existing standards needs to be known. They have been covered in chapter 3. It is known that the most critical harmonic to attenuate is the one located at $f_{sw} - 2f_g$ [31], where f_{sw} is the switching frequency and f_g is the fundamental (grid) frequency. From the known voltage harmonics covered in chapter 2 and the current amplitude limit 0.6 % of high order harmonics regulated by IEC 61000-3-4 [32], the needed attenuation can be found.

The 50 kW charger has a rated current of 73 A. With said harmonic amplitude limit, 0.6 % of the rated current, the maximum allowed amplitude for high order harmonics is $0.006 \cdot 73\ A = 0.438\ A$. The transfer function of the filter needs to attenuate all current harmonics below this level.

In order to find the desired attenuation, the amplitude of the voltage harmonics causing the currents needs to be known. A simulation of a three

phase voltage generated with SPWM modulation is set up and shown in figure 4.1. The chosen dc link voltage for the converter is 700 V and the modulated peak voltage is approximately 326 V, giving a modulation index of $M \approx 652/700 \approx 0.93$.

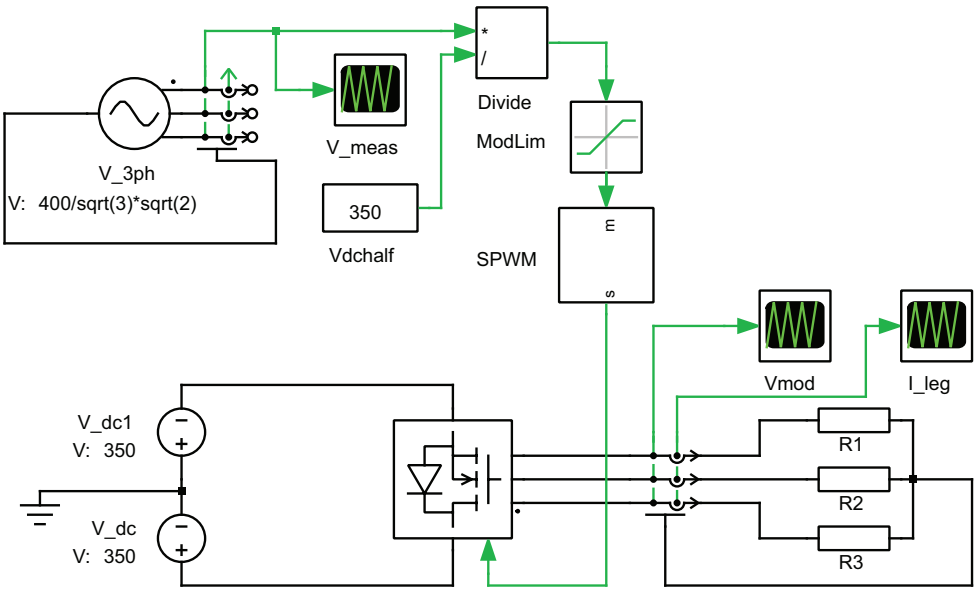

Figure 4.1: PLECS circuit for testing harmonic content of modulated signals.

The spectra of the modulated voltage at a phase leg is shown in figure 4.2. It shows that the amplitude of the voltage at the first switching frequency is 99.6 V. The root mean square (RMS) value is 70.4 V. The attenuation can then be found as $\frac{0.438\ A}{70.4\ V} \approx 0.0062\ A/V$. This is the minimum attenuation needed in order to fulfil the harmonic requirements.

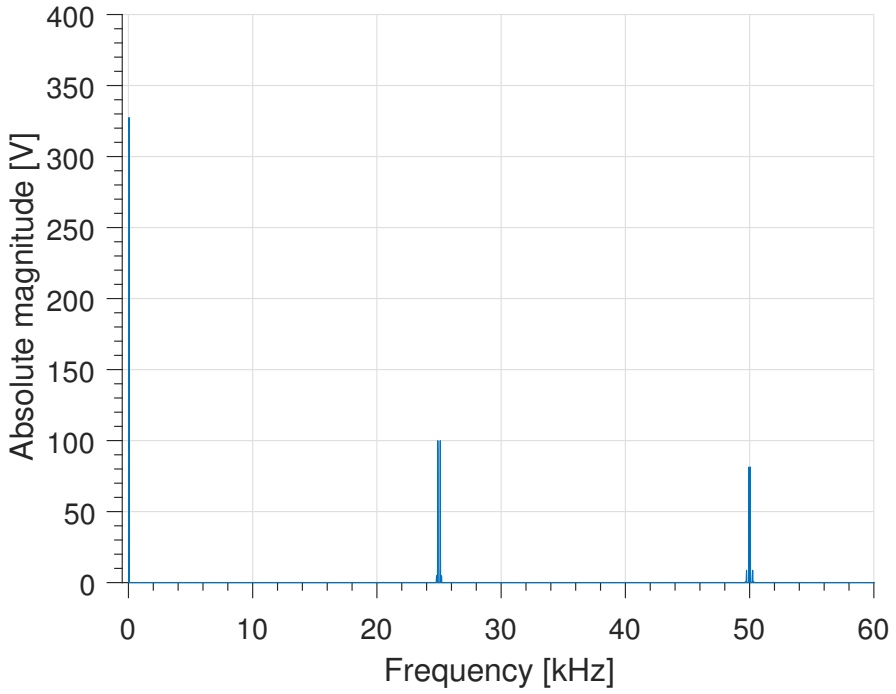

Figure 4.2: Harmonic spectra of the modulated phase leg voltage.

When later on, the interleaving operation is investigated, the harmonics surrounding the switching frequency are cancelled out. This leaves the harmonics at twice the switching frequency to be the most significant. When designing the filter for interleaved operation, it is assumed that those harmonics are of similar size as in normal operation, which leaves it around 57.3 V_{rms}. The required attenuation would then be $\frac{0.438\ A}{57.3\ V} \approx 0.0076\ A/V$ at 50 kHz, hopefully reducing the size of the filter solution significantly.

4.2 L-filter

The simplest form of low pass filter is a single series connected inductor. This type of of first order filter provides an attenuation of 20 $dB/decade$ which in some applications works well, but for high power and good suppression of harmonic content, tends to increase in both weight and size to provide satisfactory attenuation [33].

4.3 High order filters, LCL-filter

The LCL-filter, for which theory is previously described more in detail in section 2.6.2, provides a unique opportunity to achieve reduced filter size and weight compared to the simpler L-filter [7]. This higher order filter provides possibilities for high attenuation, but bad filter design can also cause interference with the converter. Using a higher order filter such as the LCL-filter introduces extra design considerations, for example: impact on power factor, resonance and control issues.

The design procedure adapted for this thesis is mostly based on [3], [6] and is described in detail in this section. The design steps will be followed and, at times, expanded analysis and implication of made parameter choices is provided. This includes comments on resonance damping losses.

A circuit of a grid connected active rectifier with LCL filtering is illustrated in figure 4.3. The filter inductances are referred to as grid side inductor, L_g, and converter side inductor, L_s. The filter capacitor C_f is star connected in series with the damping resistor, R_d.

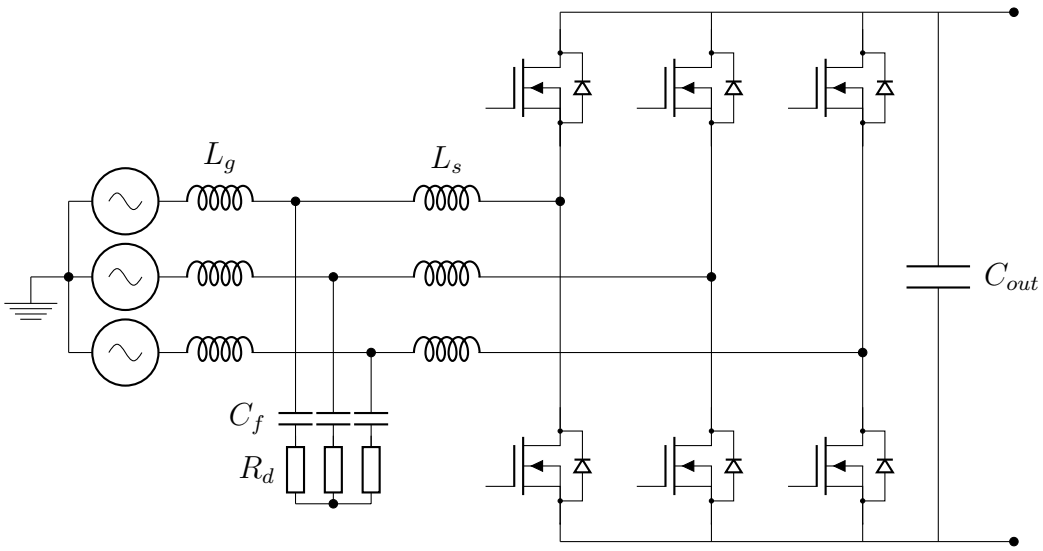

Figure 4.3: Active MOSFET rectifier with input LCL-filter.

4.3.1 Design methodology of LCL-filter

For this thesis, the initial filter design is done by following an already proposed design methodology. The resulting filter properties is later compared to the needs of the 50 kW charger, after which parameter tuning is performed. As suggested in [3], the choice of the filter capacitor C_f affects the power factor of the rectifier as perceived by the grid. Limiting the effect

the capacitor has on the power factor is the first design constraint. The power factor depends both on the choice of capacitor and later inductor values. The constraint is set up as $C_f = C_B C_{\%,max}$, where C_B is the base capacitance defined as

$$Z_B = \frac{V^2}{P_n} \qquad \Rightarrow \qquad C_B = \frac{1}{\omega Z_B} \tag{4.1}$$

in which, V is the grid voltage, P_n is the rated power of the converter, Z_B is the base impedance, and ω is the grid frequency in radians [6]. The maximum capacitor value is chosen to a percentage of the base capacitance, for example 5 % $\Rightarrow C_{\%,max} = 0.05$.

The converter side inductor, L_s, is chosen to get desired attenuation of the maximum current ripple, $\Delta I_{L_s,max}$. According to [34], the maximum ripple can be expressed as

$$\Delta I_{L_s,max} = \frac{V_{DC}}{6 f_{sw} L_s} \tag{4.2}$$

where V_{DC} is the dc link voltage and f_{sw} is the switching frequency. The maximum current is

$$I_{max} = \frac{P_n \sqrt{2}}{3 V_{ph}} \tag{4.3}$$

By combining it with (4.2) and given ripple maximum of for example 15 %, $\Delta I_{max} = 0.15 I_{max}$, gives a converter side inductor value of

$$L_s = \frac{V_{DC}}{6 f_{sw} I_{L_s,max}} \tag{4.4}$$

The grid side inductor desired value is described in [6] as

$$L_g = \frac{\sqrt{\frac{1}{k_a^2}} + 1}{C_f \omega_{sw}^2} \tag{4.5}$$

where k_a is the desired attenuation.

When the inductor and capacitor values are calculated and chosen, the resonant frequency found in [3] as

$$f_{res} = \frac{1}{2\pi}\sqrt{\frac{L_1 + L_2}{L_1 L_2 C_f}} = \frac{\omega_{res}}{2\pi} \tag{4.6}$$

is checked to satisfy the condition

$$10 f_0 < f_{res} < \frac{1}{2} f_{sw} \tag{4.7}$$

If the condition from (4.7) holds, the damping resistor is calculated as

$$R_d = \frac{1}{3\omega_{res} C_f} \tag{4.8}$$

for a star configuration. When all the component parameters are chosen, visual inspection of BODE diagrams and simulation testing is urged in order to get a sense of if the design is successful. The design process is executed in the following section.

4.3.2 Application of LCL-filter design methodology

The previously described method is used to design a filter for the 50 kW charger of the thesis. The charger parameters are found in table 4.1.

Table 4.1: Given parameters for 50 kW charger

Parameter	**Acronym**	**Value**
Rated power	P_n	50 kW
Grid voltage	V_{LL}	400 V
Grid frequency	f_g	50 Hz
DC voltage	V_{DC}	700 V
Switching frequency	f_{sw}	25 kHz
Base impedance	Z_B	3.2 Ω
Base capacitance	C_B	995 μF

From using (4.2)-(4.4), $\Delta I_{max} = 0.15 I_{max}$ and the parameters from table 4.1, the converter side inductance is calculated to $L_s = 305\ \mu H$. A relatively

close value, 266 μH is chosen, since such an inductor of appropriate current rating is available in the laboratory for potential future lab setups.

Using the proposed capacitance limit of maximum 5 % of the base capacitance, the maximum capacitor value is 50 μF. The closest commercial value from the E-12 serie is 47 μF, and is used for further calculations.

With the desired attenuation set as $k_a = 0.2$, the grid side inductance is found through (4.5), as $L_g = 5.4\ \mu H$. Since inductors of this high current ratings are usually not available and have to be custom ordered, a value of 5 μH is chosen for simplicity.

The resulting resonance frequency from (4.6), is $f_{res} = 10\,479\ Hz$, which satisfies the boundaries given in (4.7). The damping resistor is calculated using (4.8), as $R_d = 0.1\ \Omega$.

In order to get a sense of what the resulting filter attenuation is, and how the different parameter choices affect the transfer function, bode diagrams for different parameter choices are plotted and explained. A bode diagram for different resistor values is shown in figure 4.4. The figure supports the theory with a lower resistance increases the risk of resonance but on the other hand the attenuation curve is steeper above the cut off frequency. On the opposite case, with increasing resistance, the resonance peak is damped at the cost of a less attenuation above the cut off frequency, as well as increased losses.

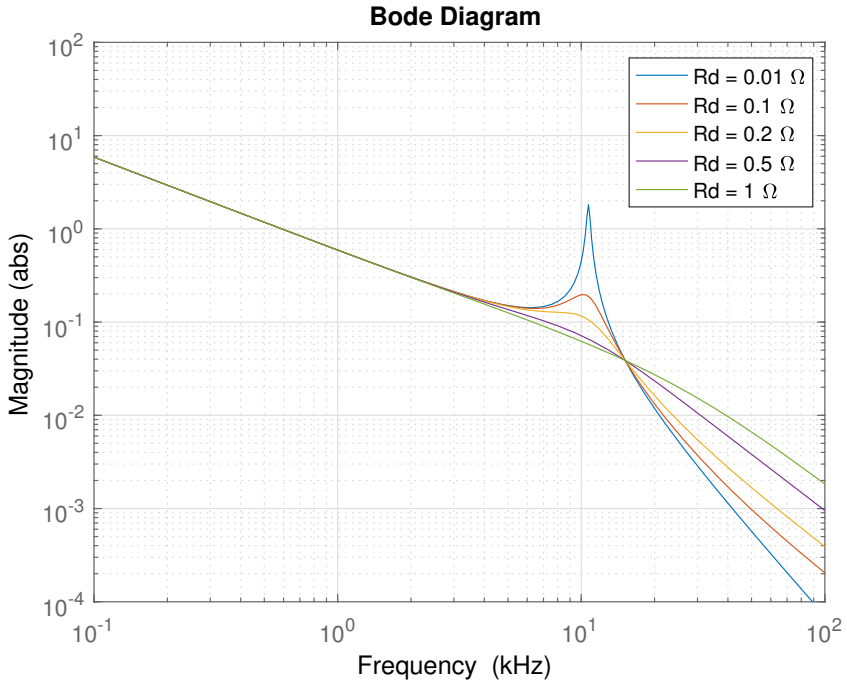

Figure 4.4: Bode diagram of an LCL filter attenuation for different values of damping resistor R_d. $L_s = 266\ \mu H, L_g = 5\ \mu H, C_f = 47\ \mu F$

Zooming in on the attenuation for the proposed choice of parameter ($R_d = 0.1\ \Omega$) it can be seen that at the switching frequency, the attenuation is 0.00625. This is very close to what is needed to suppress the theoretical maximum ripple sufficiently (0.0062, found in section 4.1). Some margin is usually desired, and a way of increasing the attenuation needs to be found. Equation (4.5) hints that a higher demand on attenuation can be fixed by choosing a higher value for the grid side inductor L_g. In order to be able to visually evaluate how a higher grid side inductance affects the transfer function, the bode diagram is plotted for a few selected values of L_g and is shown in figure 4.5. From the diagram it can be seen that increasing the grid side inductance lowers the resonance frequency and cutoff frequency, yielding better attenuation at the critical harmonic. The attenuation at 25 kHz now reads as 0.0028 for $L_g = 10\ \mu H$, giving a satisfactory margin.

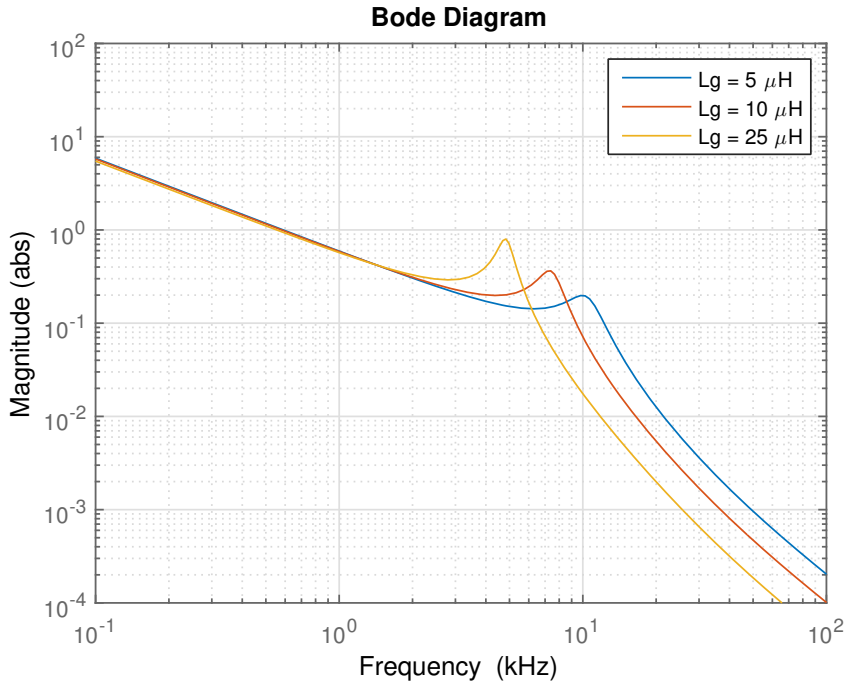

Figure 4.5: Bode diagram of an LCL filter attenuation for different values of grid side inductor L_g. $L_s = 266\ \mu H, C_f = 47\ \mu F, R_d = 0.1\ \Omega$.

All the resulting filter parameter values are presented in table 4.2.

Table 4.2: Resulting filter parameters for normal operation.

Parameter	Acronym	Value
Converter side inductance	L_s	266 μH
Grid side inductance	L_g	10 μH
Filter capacitance	C_f	47 μF
Damping resistor	R_d	0.1 Ω

4.4 Interaction with grid inductance

When placing the converter with its filter in a grid, the impedance of the grid will add to a total transfer function. The inductance of the grid is series connected with the grid side inductance of the filter and will behave as such, the inductances values adding together.

Simulations are made with different grid inductances. The locations in the grid are selected in such a way that their impedance was meant to represent locations with a large variety of resistance and inductance but in reality the values was surprisingly similar, both the resistance and the inductance differed for example less than a factor 4 between the strongest and the weakest location.

The highest value for grid inductance L_k was 124 μH, roughly 10 times the value of the grid side inductance selected for the 50 kW charger. In order to get a sense of what the grid inductance does to the total transfer function, the bode diagram for different total grid side inductance is plotted and shown in figure 4.6. The resonance and cut-off frequency gets lower for higher grid side inductances. Considering this fact, the filter should be able to be designed to just have the needed attenuation, and any extra inductance from the grid is seen as a bonus giving an extra desired margin.

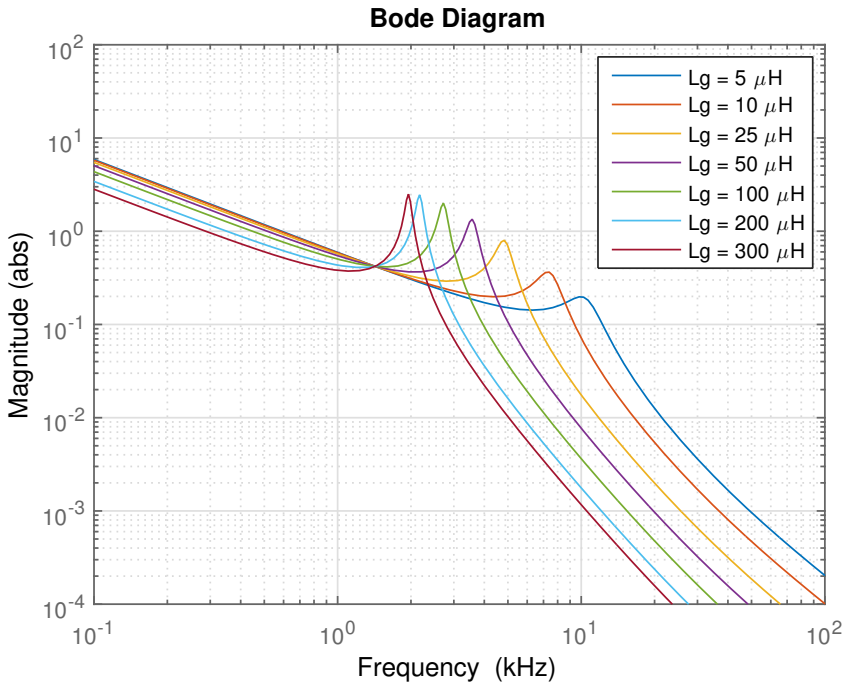

Figure 4.6: Bode diagram of an LCL-filter attenuation for different values of grid side inductor L_g. $L_s = 266\ \mu H, C_f = 47\ \mu F, R_d = 0.1\ \Omega$.

5

Modeling of three-phase rectifiers

All electric equipment will affect the grid it is connected to, electric power converters makes no exception. With voltage control of power electronic equipment, the high frequency switching will be followed by undesirable harmonic output [35]. To understand the behaviour of such a converter and how to prevent unwanted EMI a simple model is developed and compared to the bus charger described in previous chapters.

This chapter aims to, by creating a model, represent the Siemens rectifier covered in chapter 3. The simulated results can be compared to the actual measured values. The additional converter, with rated power of 50 kW and switching frequency of 25 kHz, is then developed and modelled from previous experiences. Instead of galvanically isolating by using a transformer on the grid side, as in the Siemens case, the galvanic isolation could be accomplished by having a high frequency DC/DC converter on the secondary (battery) side.

The 50 kW charger is then simulated to operate interleaved. The interleaved model and controller changes is covered in the end of this chapter.

5.1 Setting up a system model environment

A circuit is designed representing a 3-phase voltage source with a grid equivalent impedance, a filter circuit, a converter and a load. The different covered solutions are modelled in PLECS® blockset from Plexim and is run from a Simulink/MATLAB® environment. The controller for each model is built entirely in PLECS. Each converter model is covered in the following sections.

5.2 Chosen control method

A closed loop controller is needed to run simulations of the different rectifiers. Since the frequency content analysis is made in steady state, the control design in this thesis will not play a big role. No great emphasis will be put into giving the system a good response. Instead a simple and straight forward controller design method found in [5], [36] will be partly adopted.

The voltage source, voltage control method is adapted in this thesis. The block diagram for the system setup is seen in figure 5.1, and refers to the circuit in figure 2.5 from chapter 2. $G_c(s)$ and $G_v(s)$ are the physical responses for the line current and dc voltage [5]. $F_c(s)$ and $F_v(s)$ are the voltage and current controllers, respectively.

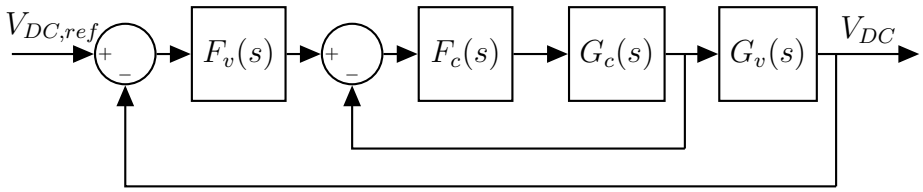

Figure 5.1: Block diagram for voltage oriented control.

The physical responses $G_c(s)$ and $G_v(s)$ can be written as

$$G_c(s) = \frac{1}{sL_s + R_{L_s}} \qquad G_v(s) = \frac{3V_{ph}}{sC_{out}} \tag{5.1}$$

where V_{ph} is the RMS phase voltage the rectifier is connected to, C_{out} is the dc link capacitor, L_s is the converter side inductor and R_{L_s} is the series resistance of L_s. Proportional and intergrating (PI) controllers are designed for both the dc voltage and line current.

The voltage controller is a PI controller with anti windup. The current controller has cross coupling, feed forward and anti windup. The block diagram of each controller can be found in appendix A. The controller parameters are presented in respective converter description throughout the chapter, with the methods of retrieving them also presented in the appendix.

5.3 Model of the Siemens charger

An interpretation of how the Siemens charger is constructed lead to the circuit presented in chapter 3. When realising the model, some unknown component values and functionality have to be estimated as good as possible. The resulting simulation model is shown in figure 5.2.

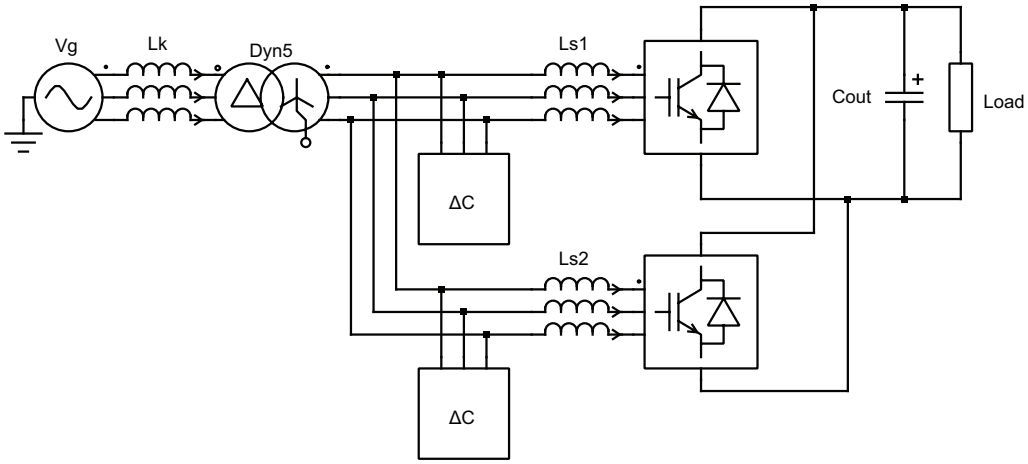

Figure 5.2: Simulation model of the Siemens charger

Regarding the unknown filter connected on the grid side of the transformer, it has been assumed to be an EMI filter of some sort. The effect it shows on the performed measurements are minimal and therefore it is chosen to be excluded from the model entirely.

The transformer is modeled as Dyn5 with a winding ratio of 3:1. The only other available parameters are the impedance z_k of 5.8 % and the rated capacity of 400 kVA. The estimated efficiency for such a transformer is 99 %. The only losses in the simulation transformer model are resistive losses. All the resistive losses is modeled to be on the converter side of the transformer. At rated load, that would yield 4 kW losses.

The resistive transformer losses are from these conditions described by

$$P_{T,loss} = 3R_T(\sqrt{3}I_{rated})^2 = 4\ kW \tag{5.2}$$

where I_{rated} is the rated current on the grid side of the transformer and R_T is the transformer series resistance. The rated current is calculated as

$$I_{rated} = \frac{P_{T,rated}}{\sqrt{3}V} = \frac{400\ kW}{\sqrt{3}\cdot 400\ V} \approx 577\ A \tag{5.3}$$

where V is the grid voltage. Combining (5.2) and (5.3) gives the transformer resistance as

$$R_T = \frac{4\ kW}{3(\sqrt{3} \cdot 577)^2\ A} = 1.3\ m\Omega \tag{5.4}$$

A series inductance is added, as a part of the transformer, on the converter side to model the inductance of the transformer. Its value is chosen to 50 μH. The value was found by fitting the harmonic results of the simulations to the performed measurements on the system.

The value of the output capacitor C_{out} is unknown, and is chosen as 1000 μF, which is a commercially available DC capacitor value.

The IGBTs are modelled with a forward voltage drop and a purely resistive voltage drop over the channel. The anti-parallel diode is modelled in the same manner. A pre-designed IGBT converter module is used in PLECS. The values were decided by looking up an IGBT with similar ratings and retrieving the parameters from its data sheet. Ideal switching is considered, with no blanking time.

The capacitor and input inductor values were set as found in chapter 3. The internal resistance of the inductor is unknown and is estimated to 5 $m\Omega$. 1 Ω is chosen for the capacitor series resistance, in order to damp potential resonance.

The load is chosen as $R_{load} = 1.9\ \Omega$ in order to achieve the same load level, $P_{out} = 240\ kW$, $V_{DC} = 675\ V$, as where the measurements were made.

5.3.1 Control of Siemens charger

No adequate information on the Siemens charger control is available in its corresponding documentation nor have any attempts with email correspondence been successful. In order to be able to simulate the system, a simple voltage and current controller is constructed. Following the methodology from section 5.2, the following parameters were found. α_c and α_v are the controller bandwidths, K_{pc} and K_{pv} are the current and voltage controller proportional gains, and K_{ic} and K_{iv} are the controller integral gains.

$$\alpha_c = \frac{\omega_{sw}}{10} \approx 1885 \qquad \alpha_v = \frac{\alpha_c}{10} \approx 188.5 \tag{5.5}$$

$$K_{pc} = \alpha_c \frac{L_s}{2} \approx 0.5655 \qquad K_{pv} = \frac{\alpha_v C_{out}}{\sqrt{3} V_{ph}} \approx 0.00058 \tag{5.6}$$

$$K_{ic} = \alpha_c R_{L_s} \approx 9.42 \qquad K_{iv} = \alpha_v K_{pv} \approx 0.11 \tag{5.7}$$

A block diagram illustration of the controller implemented in PLECS is shown in figure 5.3. A phase locked loop (PLL) is connected at the converter side of the transformer in order to estimate the voltage amplitude and phase. The PLL bandwidth is set to 25 Hz. The controller block contains the voltage and current controller. Because of voltage harmonics found from measurements, it is estimated that symmetrical SVPWM is used. A PLECS block for SVPWM is therefore used to generate the transistor gate signals. The switching frequency, f_{sw}, is 3 kHz.

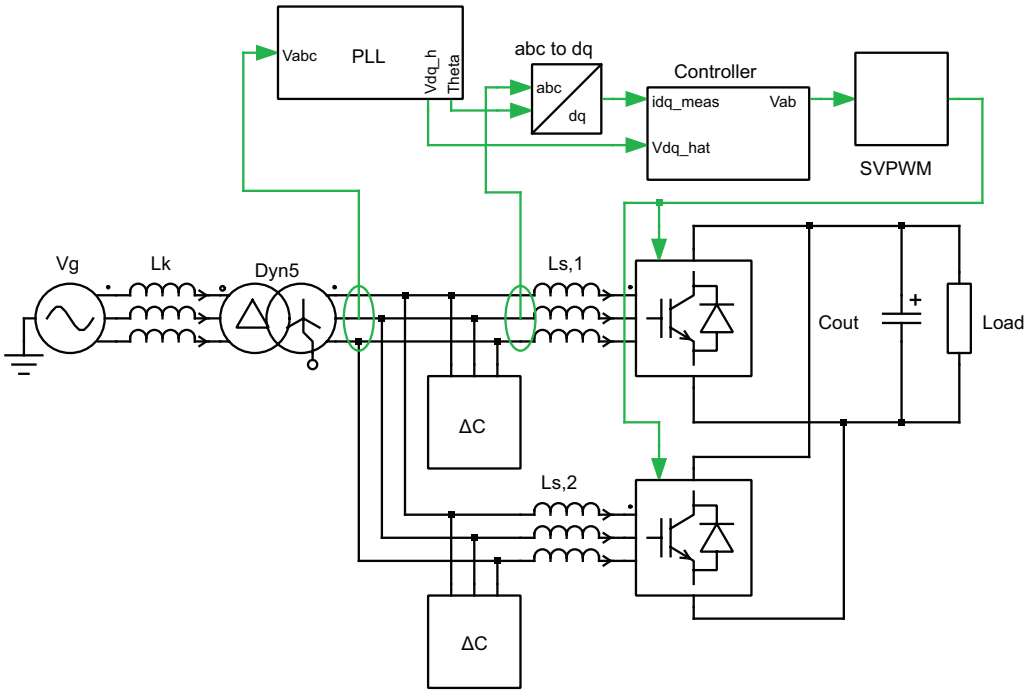

Figure 5.3: Siemens charger with control blocks and sensor positions.

5.4 Model of 50 kW charger

The 50 kW model is modelled with silicon carbide (SiC) MOSFETs instead of IGBTs. SiC-MOSFETs have low rise and fall times which means they have lower losses per switch event. As a result of this, higher switching frequencies can be utilised without suffering high losses. The target switching

frequency in this thesis is 25 kHz, which puts it outside of the hearing range (roughly 20 $Hz - 20\ kHz$).

As opposed to the Siemens charger covered in this thesis, the 50 kW charger is not parallel in any way in its original behaviour. As shown in figure 5.4, it consists of a single LCL-filter and a converter stage. Instead of using a transformer for galvanic isolation, a high frequency DC/DC converter can be used on the dc link.

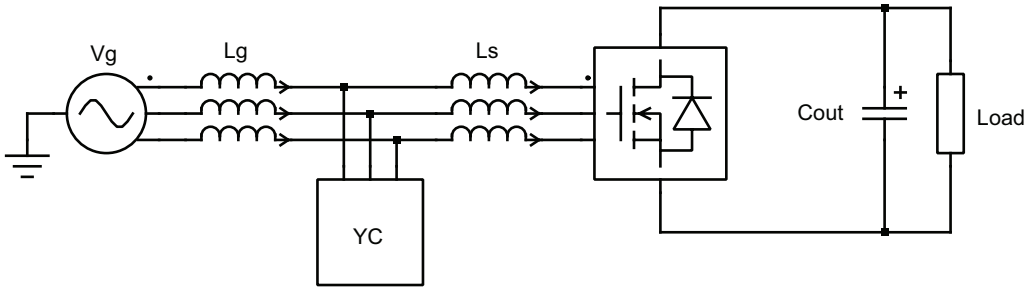

Figure 5.4: Circuit model of active MOSFET rectifier with input LCL filter.

5.4.1 50 kW charger interleaved operation

There are different ways of implementing interleaved converter design. The most beneficial would be if the phase legs of the two converters were connected to each other, and sharing the LCL-filter all together, but it is unfortunately not that simple. The phenomenon of circulating currents needs some impedance in the mesh in order not to get out of hand. A few different ways of connecting interleaved converters is shown in [11]. The method chosen for the 50 kW rectifier is duplicating the converter side inductor, but dividing the inductance value in half, to $L_{s,1} = L_{s,2} = 133\ \mu H$.

The scheme is shown in figure 5.5. The current can now split between the converters, and the component ratings can be reduced. The grid side inductors $L_{s,1}$ and $L_{s,2}$ limits the circulating current, ensuring stable operation of the rectifier. This configuration does not have the same transfer function as the LCL-filter during normal operation. The filter design methodology is therefore not applicable in the same way.

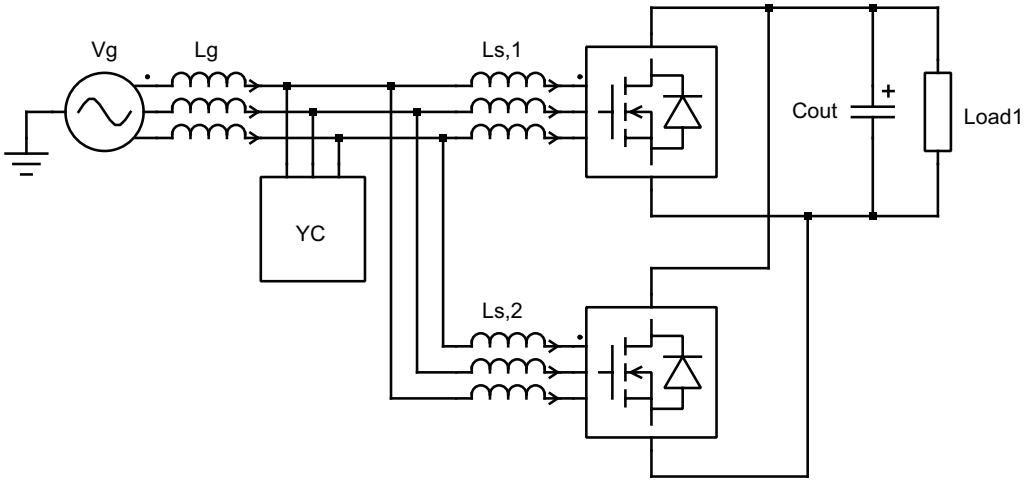

Figure 5.5: Active MOSFET rectifier circuit for interleaved operation.

5.4.2 Control of 50 kW charger

In the same manner as for the Siemens charger model, a voltage oriented control is implemented. The parameters are deduced in the same way, not considering the extra LC added too the input circuit.

$$\alpha_c = \frac{\omega_{sw}}{10} \approx 15708 \qquad \alpha_v = \frac{\alpha_c}{10} \approx 1571 \tag{5.8}$$

$$K_{pc} = \alpha_c L_s \approx 4.18 \qquad K_{pv} = \frac{\alpha_v C_{out}}{3V_{ph}} \approx 0.0009 \tag{5.9}$$

$$K_{ic} = \alpha_c R_{L_s} \approx 78.5 \qquad K_{iv} = \alpha_v K_{pv} \approx 1.39 \tag{5.10}$$

The controller is implemented as shown in figure 5.6. The input current is measured by the converter side inductor L_s, and the input voltage is measured before the grid side inductance L_g.

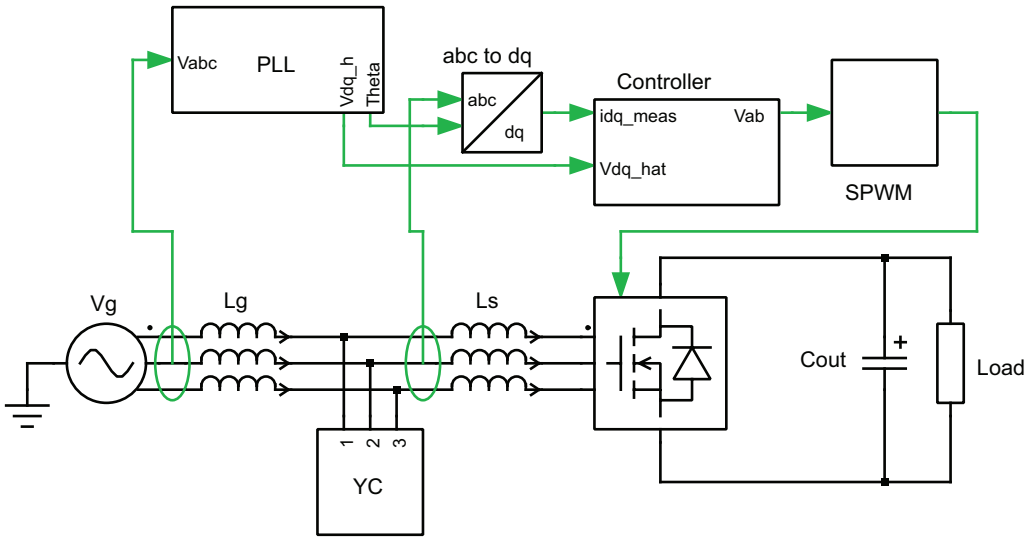

Figure 5.6: 50 kW charger with control blocks and sensor positions.

5.4.2.1 Interleaving operation controller changes

The estimated converter side inductance is now 133 μH, resulting in a proportional gain of $K_{pc} = 2.09$. Otherwise the controller performance is the same, the only exception being where the current is measured. The feeding voltage is measured at the same position as in normal operation, before the grid side inductance. The current is measured in the same way as for the paralleled converter stages in the Siemens model, at one of the converter side input inductors.

5.5 Model parameters

A list of model parameters for the two converter solutions are shown in table 5.1. The controller parameters are presented in respective converters control section.

Table 5.1: Simulation model parameters.

Shared parameters		
Parameter	**Acronym**	**Siemens & 50 kW**
Grid main voltage	V	400 V
Grid frequency	f_g	50 Hz

Filter parameters			
Parameter	**Acronym**	**Siemens**	**50 kW**
Converter side inductance	L_s	600 μH	266 μH
Grid side inductance	L_g	50 μH	10 μH
Filter capacitance	C_f	66 μF	47 μF
Damping resistance	R_d	1 Ω	0.1 Ω

Converter parameters			
DC capacitance	C_{out}	1000 μF	320 μF
Transistor on resistance	R_{ON}	7 $m\Omega$	5 $m\Omega$
Transistor forward voltage	V_f	1.5 V	-*
AP diode on resistance	$R_{D,ON}$	3.4 $m\Omega$	2 $m\Omega$
AP diode forward voltage	$V_{D,f}$	1.3 V	2 V

Load parameters			
Load resistance	R_{load}	1.9 Ω	9.8 Ω

** The MOSFET does not have any forward voltage drop.*

6

Results

In this chapter results from performed measurements and simulations are presented. Firstly, the measurement results of the Siemens charger are presented and are compared with the simulation results on the same converter. Simulation results of the 50 kW charger is then presented, as well as the interleaved operation results. Finally, the size reduction achieved by going from normal to interleaved operation is presented in brief.

6.1 Measurement results from field measurements at 300 kW bus charger

In this section, voltage quality such as harmonic content at the grid connection point of the 300 kW charger is presented. Then an overview of the charging cycle and steady state efficiency values is presented for different load levels. Lastly the harmonics of both drawn current and supplied voltage during high load is examined and presented.

6.1.1 Idle voltage quality

When the charger is in stand-by mode, with its pantograph in upper (disconnected) position, currents and voltages are measured at the node where the charger setup is connected to the grid. Idle grid voltage and current waveforms at grid connection point are presented in figure 6.1. It is visible from the figure that a current is drawn despite that the charger is in idle mode. This idle current might be used to, for example, drive the control circuit of the converter and, due to the magnitude, is possibly a minor contributor to the harmonic content of the idle voltage. It can visually be seen in figure 6.1 that there are other frequency components (low order harmonics) distorting the supplying voltage.

The current drawn is obviously not sinusoidal shaped but fairly small com-

pared to the current during charging. Since disconnection of the device is not an option, this is the best point of reference that can be given when later making comparisons.

In a zoom in on the voltage in figure 6.1, other frequency components can clearly be seen as a ripple in figure 6.2. It is also worth mentioning that the voltage resolution of the 12 bit oscilloscope gets visible in this zoom as quantised voltage steps in Y-scale. The visible ripple in this zoom corresponds to harmonics in the 3 kHz and 6 kHz region which is also, as suspected, visible in the energy spectrum in the frequency domain presented in figure 6.3. The presence of frequency components in voltage in the 3 kHz region during idle is fairly surprising and opens for further investigations. Of course the converter is switching in 3 kHz but since the drawn idle current is small (about 7.6 A_{RMS}) its contribution to the comparatively large voltage harmonic is unexpected.

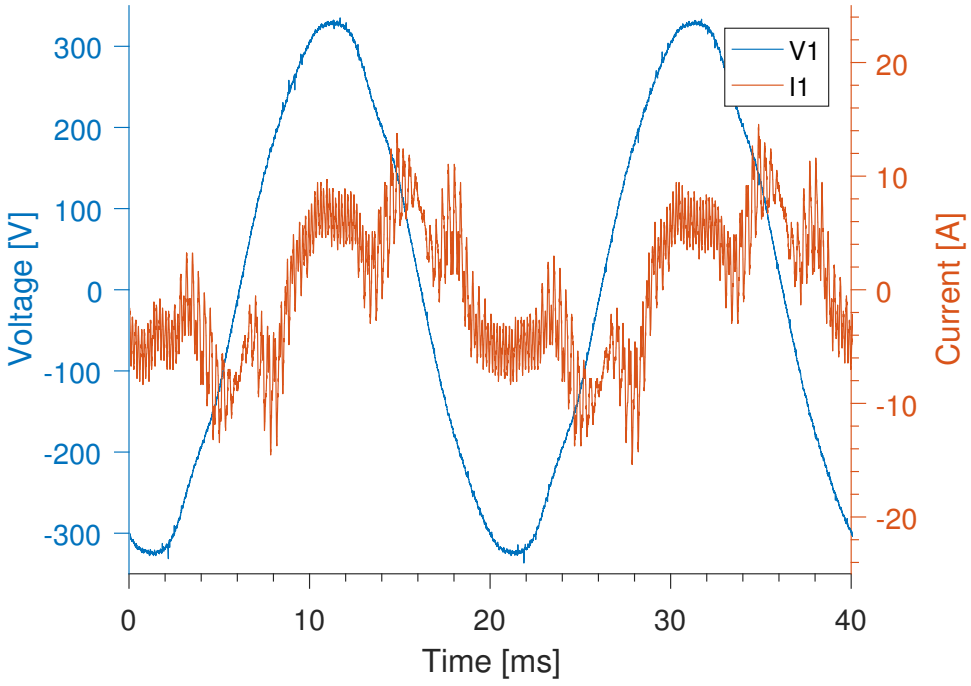

Figure 6.1: Voltage and current waveform when charger is inactive.

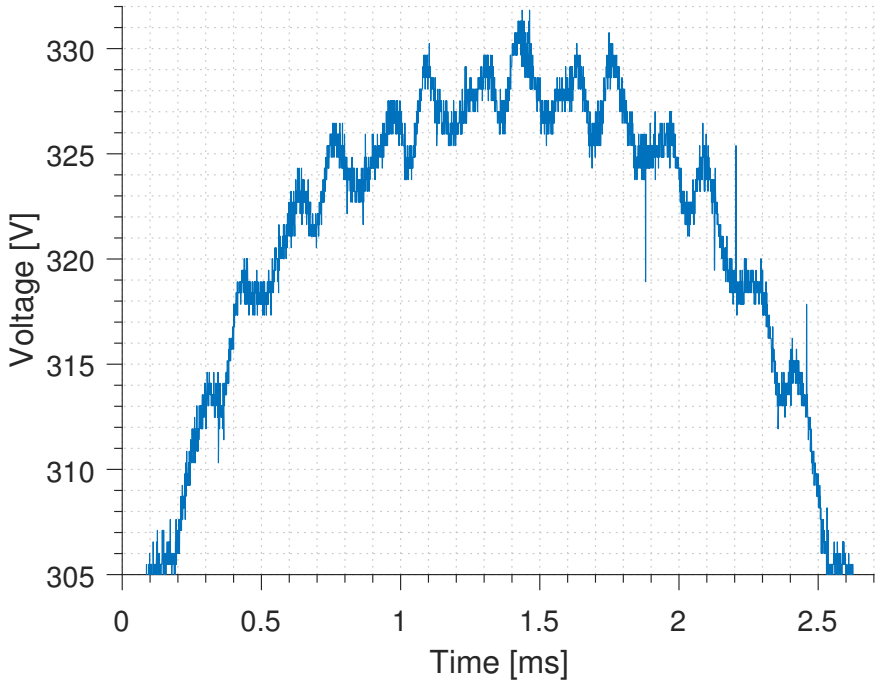

Figure 6.2: Zoom of one voltage peak during idle.

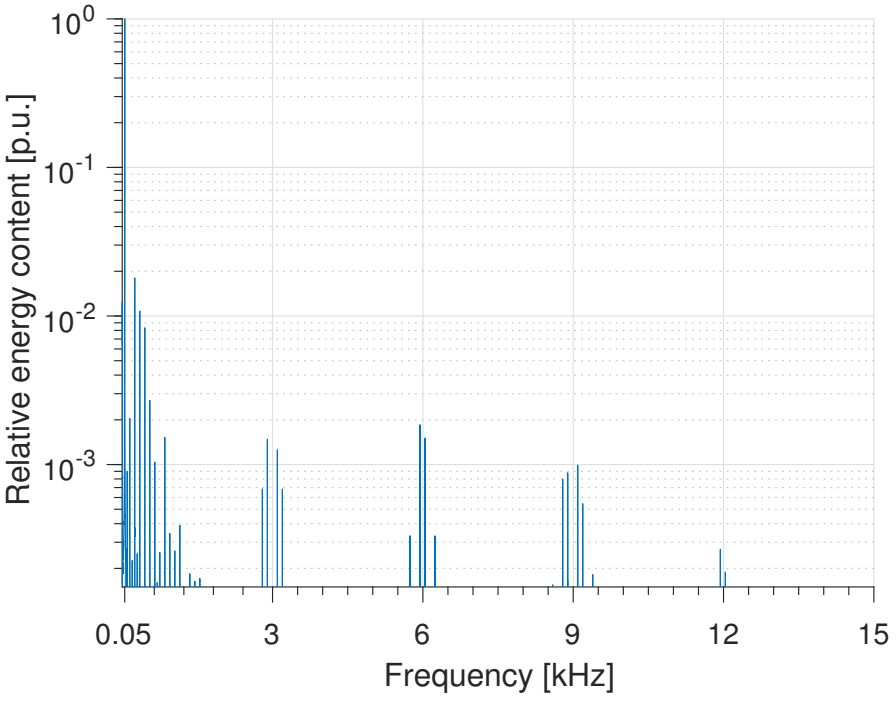

Figure 6.3: Relative energy content in voltage during idle.

The normalized measured harmonic content for idle voltage is shown in figure 6.4 and some of its numerical values are presented in table 6.1. As

mentioned earlier, there is some frequency content already present in the idle voltage, especially in the region between 50 Hz to a few hundreds of Hz. This rises suspicions whether this is coming from the feeding grid or if the converter is the source. The harmonic content is however comfortably below the limitations presented in chapter 3. In the THD-value in table 6.1, the first 40 harmonics are taken into account in accordance with [15].

The measurements taken on the charger in daily operation was performed during one single day. This means that there may be, and probably are, factors affecting the measured quantities. This can be factors as disturbances from other equipment in the grid or other stochastic factors which are not controlled or verified.

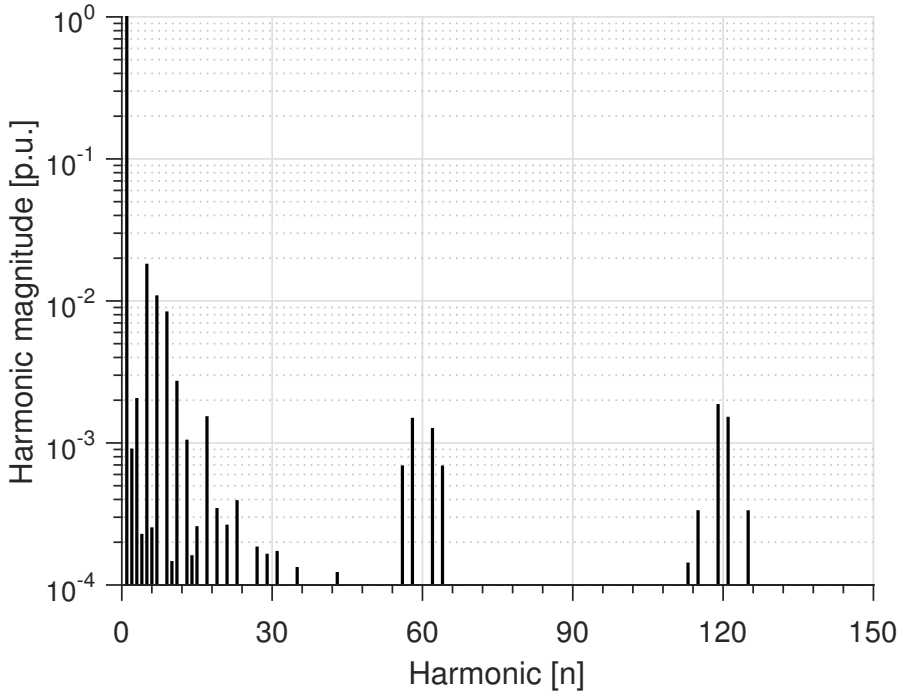

Figure 6.4: Measured harmonic content of the voltage during idle operation.

Table 6.1: Measured voltage harmonics at PCC when charger is inactive.

	Relative amplitude							[%]
	$f_{(3)}$	$f_{(5)}$	$f_{(7)}$	$f_{(11)}$	$f_{(13)}$	f_{sw}	$f_{sw,2}$	THD
Voltage (V_1)	0.20	1.80	0.11	0.27	0.10	0.15	0.19	4.9

6.1.2 Overview of charging cycle and efficiency

The charge current i_{dc} and voltage v_{dc} is captured for a full charging cycle in figure 6.5. The ramp up time is around 15 s.

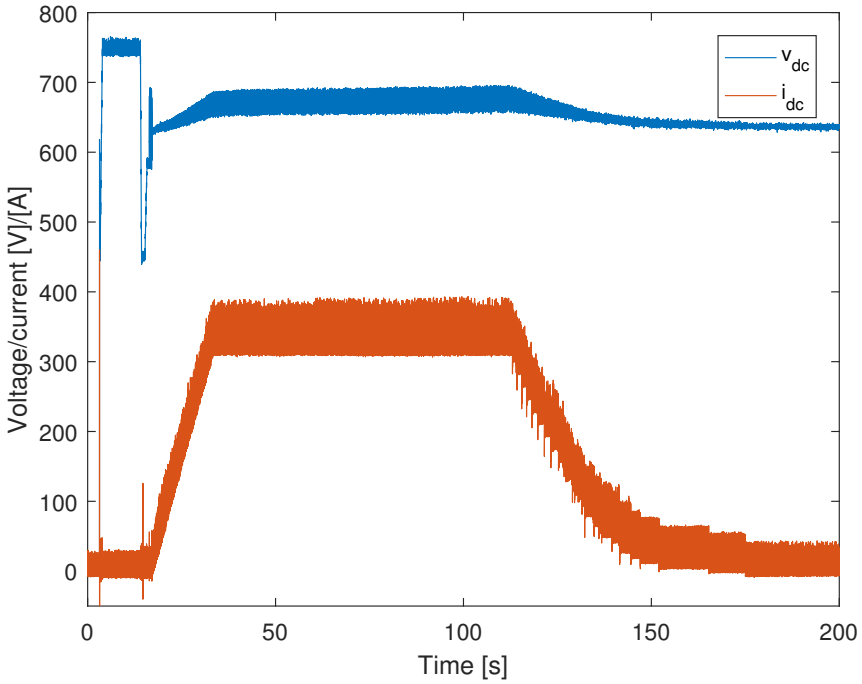

Figure 6.5: Charge cycle for an electric bus.

In steady state, the efficiency of the converter is calculated through, over a period $T = 10$ s, as

$$\eta = \frac{I_{dc} V_{dc}}{\frac{1}{T} \int_0^T \left(v_1(t)\, i_1(t) + v_2(t)\, i_2(t) + v_3(t)\, i_3(t) \right) dt} \tag{6.1}$$

where I_{dc} and V_{dc} are the averaged DC current and voltages while $v_{1,2,3}(t)$ and $i_{1,2,3}(t)$ are the instantaneous phase voltages and currents.

In table 6.2, power in, power out and efficiency for the converter are calculated and presented for a number of measurement series at different operating points.

Table 6.2: Siemens converter efficiency for different load levels.

I_{dc} $[A]$	V_{dc} $[V]$	P_{out} $[kW]$	P_{in} $[kW]$	η [%]
10.1	635.9	6.4	9.9	64.79
27.4	670.0	18.3	20.5	89.08
35.6	676.1	24.0	26.2	91.78
50.8	684.6	34.7	37.0	93.90
64.6	654.9	42.3	45.3	93.38
92.8	663.6	61.5	64.2	95.94
145.9	674.5	98.4	102.0	96.47
146.0	688.2	100.4	104.2	96.40
283.2	673.4	190.7	199.8	95.44
329.7	676.6	223.0	235.2	94.85
329.8	670.0	221.0	231.7	95.36

The calculated values for efficiency (P_{in}/P_{out}) is presented graphically in 6.6 where a curvefitted line is also presented. From this figure it is visible that the efficiency is mostly high for medium to high charging powers, the maximum efficiency occurs around 100 kW and decreasing slightly above.

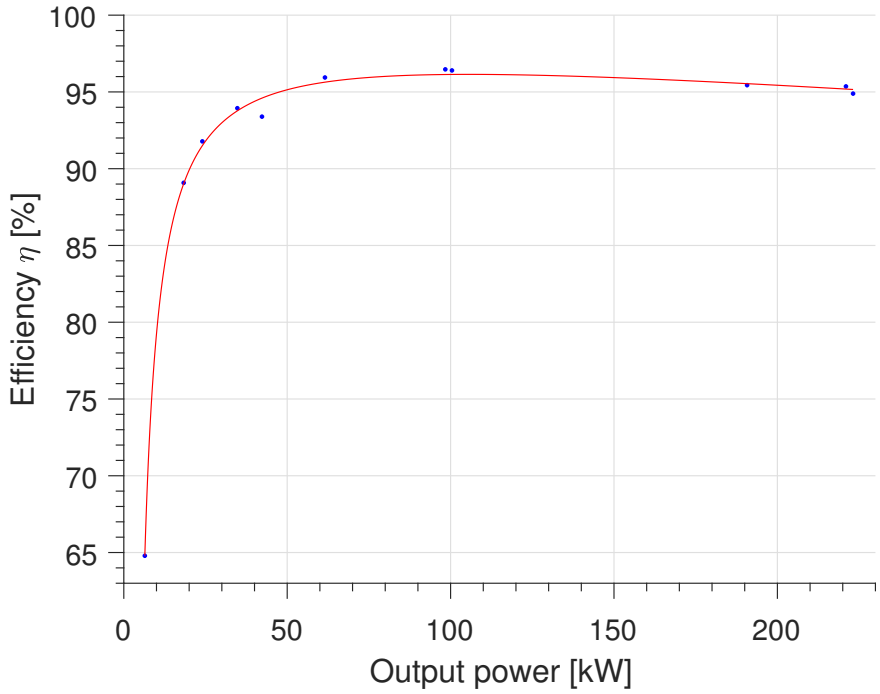

Figure 6.6: Measured efficiency as a function of load level.

6.1.3 Measured harmonic content during charge

Presented in figure 6.7 are current and voltage waveforms at the PCC. The current curve shows more sinusoidal resemblance than the voltage, suggesting that it has a smaller content of low order harmonics than the voltage. It can also be seen that the converter is operating close to unity power factor.

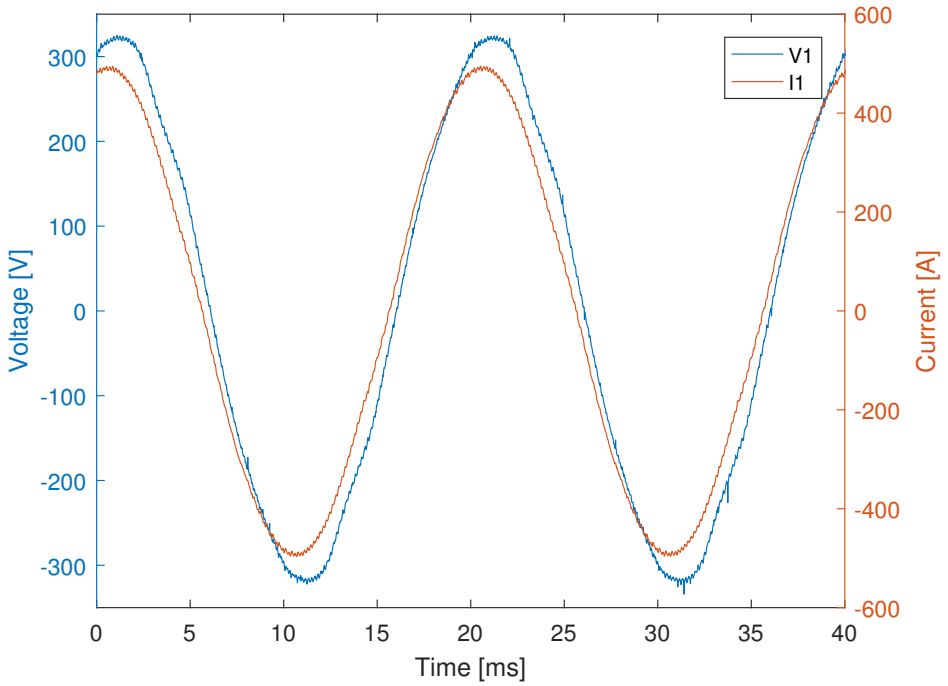

Figure 6.7: Waveforms during high load.

The frequency spectra for voltage and current during charging is presented in figure 6.8 and 6.9. The measurements at charging is performed during a 240 kW charging cycle. As indicated, the low frequency harmonic content of the current is slightly lower than that for the voltage. The Swedish regulations presented in chapter 3 are met for the current; the only harmonic above 0.5 % is the fifth, which has a limit of 6 % [15]. The IEC 61000-3-4, with a maximum limit of 0.6 % for high order harmonics, is also satisfied.

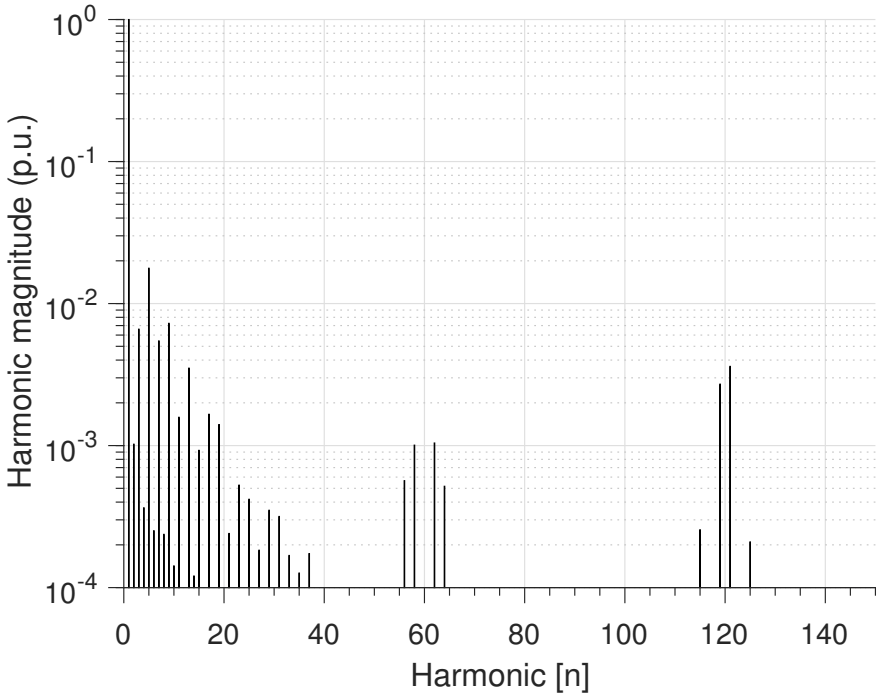

Figure 6.8: Harmonic content in voltage measured at grid connection point while charging.

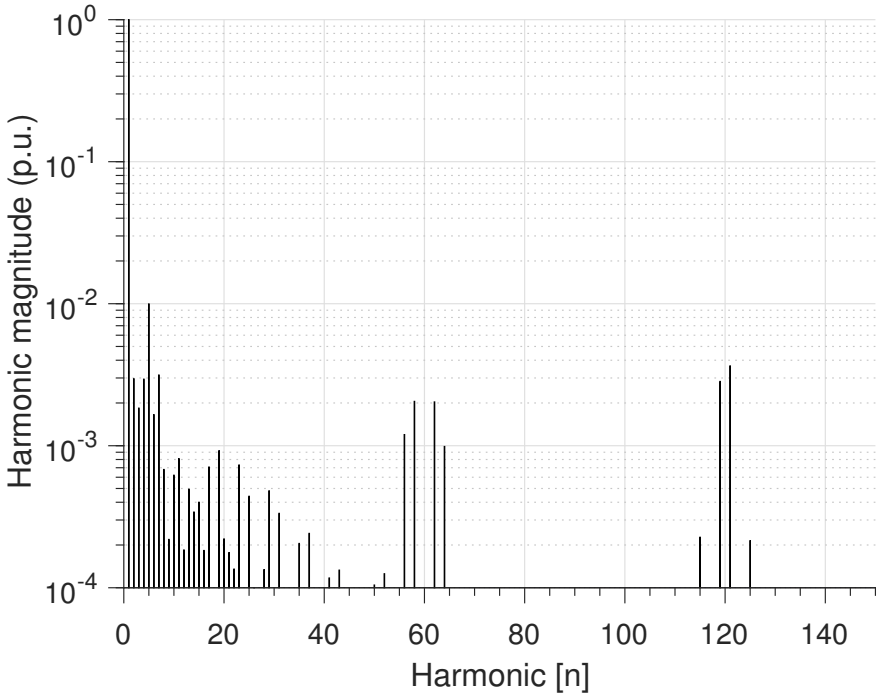

Figure 6.9: Measured harmonic content for currents drawn from grid while charging.

6.2 Results from simulation

The computer model built is tested with different parameter values and configurations. Throughout this section the simulation results from simulations are presented and commented.

The simulations presented here are performed at a load level of 240 kW. In figure 6.10, the current and voltage waveforms are presented. A close to unity power factor operation is achieved. Noteworthy is that the low order components seen in the measurements are not visible here. This is expected since the model does not contain anything that should generate significant low order components.

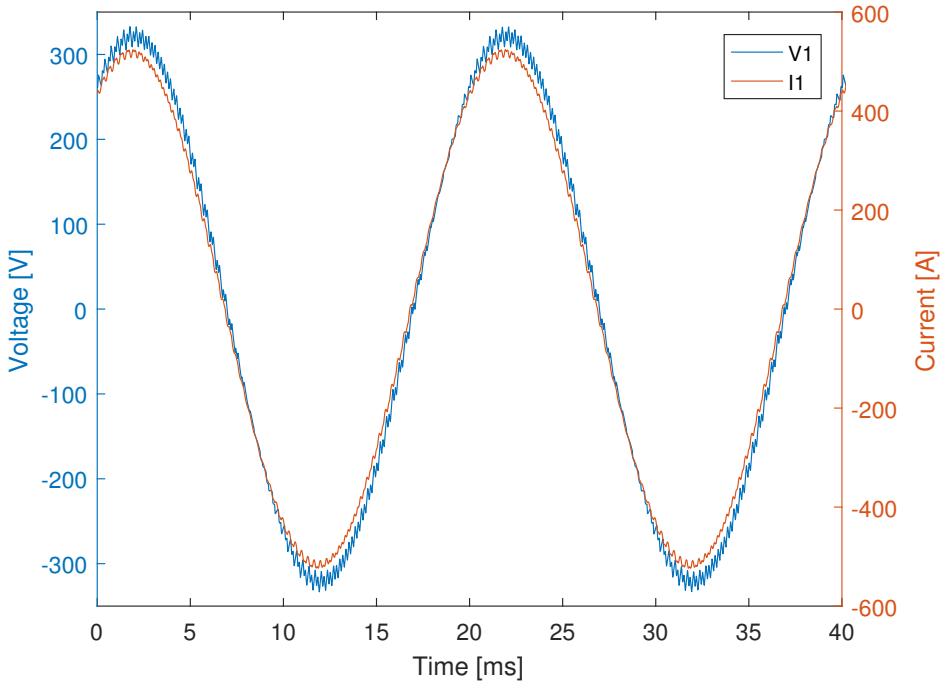

Figure 6.10: Simulated voltage and current waveforms during high load.

Presented in figure 6.11 is the harmonic content of the voltage. The harmonics at the switching frequency multiples are similar to those measured. The low order harmonics are not larger than 10^{-4} times the fundamental. Surprisingly, there are visible components at 2 and 4 times the fundamental frequency. Even order harmonics is not something that is expected to appear. The explanation for these could be a syncing mismatch between the two paralleled converter stages [37].

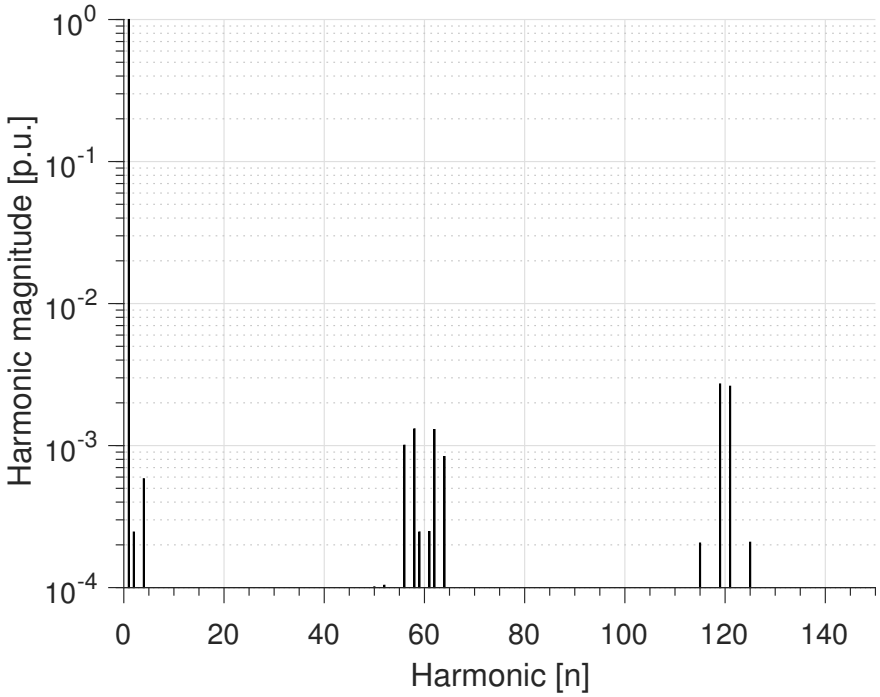

Figure 6.11: FFT of simulated voltage of model of Siemens charger with at particular Z_{sc}

The simulated current differentiates a bit more from the measurements. As seen in figure 6.12, the peaks at the switching frequency and double switching frequency are of the same amplitudes. Both are still within 2-3 times of what is measured. The difference can be caused by a number of things. Non idealities in components is one; the components in the real charger installation has a number of stray capacitances/inductances that affects the results. There is also an EMI filter on the existing charger that is disregarded in the simulations.

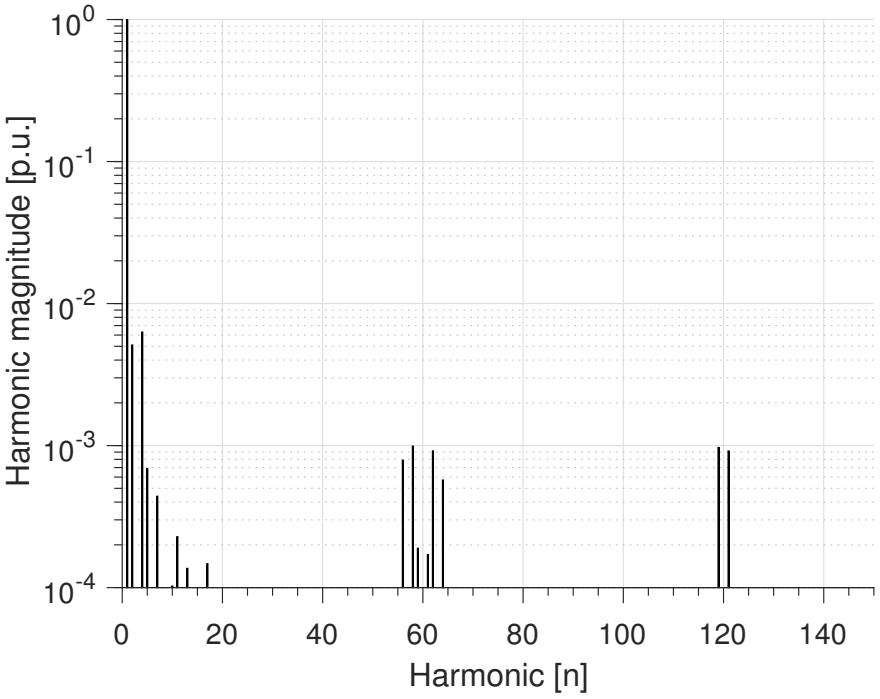

Figure 6.12: FFT of simulated current of model of Siemens charger with at particular Z_{sc}

A summary of the comparison is found in table 6.3. The amplitudes at multiples of the switching frequency make up the best match. The low order harmonics are off less interest when the filters are designed for the 50 kW charger, since the higher orders are the most critical. As a result of missing low order harmonics in the simulation, the simulated THD also differs from measured values. All of the presented values satisfy the Swedish regulations SS-EN 50160.

Table 6.3: Comparison of measured and simulated harmonics for Siemens charger during load.

Installation	**Relative amplitude***							[%]
	$f_{(3)}$	$f_{(5)}$	$f_{(7)}$	$f_{(11)}$	$f_{(13)}$	f_{sw}	$f_{sw,2}$	THD
I1 measured	0.18	0.99	0.31	0.08	0.05	0.21	0.28	4.78
I1 simulated	-	0.07	0.04	0.02	0.01	0.10	0.10	1.41
V1 measured	0.66	1.77	0.55	0.16	0.35	0.10	0.27	6.53
V1 simulated	-	-	-	-	-	0.13	0.27	0.17

**Entries marked - are less than* 10^{-4} *times the fundamental.*

6.2.1 50 kW simulated results

An initial investigation is made to see if the simulations show that the designed converter fulfills the requirements set on drawn grid current. The harmonic spectra of the phase current is shown in figure 6.13. The expected result at the switching frequency, as stated in chapter 4, is a relative magnitude of around 0.003. The resulting relative magnitude is 0.0029, a satisfactory result.

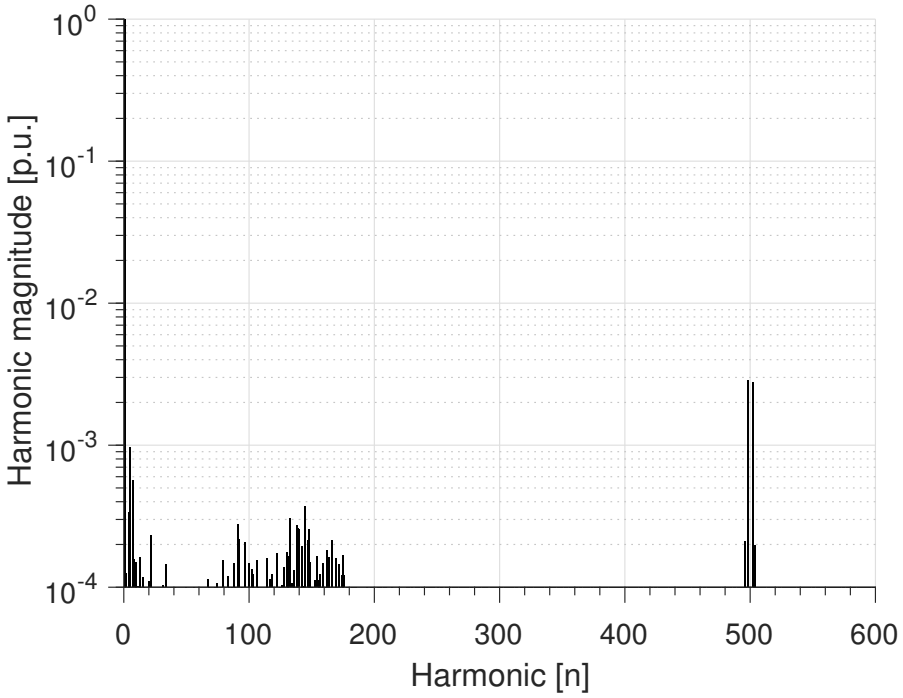

Figure 6.13: Harmonic content for currents drawn from grid (Simulation of 50 kW 25 kHz)

In figure 6.14 the voltage and current waveforms are shown in order to confirm unity power factor operation. The current and voltage is in phase, yielding a fundamental current of 73.3 A.

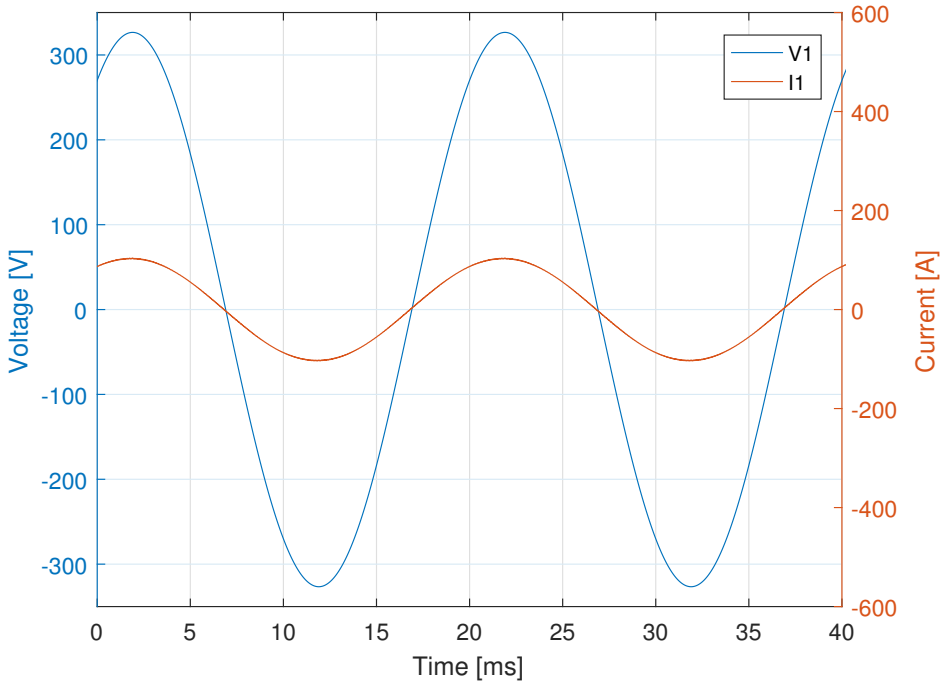

Figure 6.14: Current and voltage waveforms for 50 kW charger.

The voltage source in this case is considered perfect, therefore no harmonic content in the voltage is expected since the grid impedance is zero. Examples of simulations run with different grid impedance is presented in section 6.2.3.

6.2.2 Simulated interleaved operation results

The current harmonics of the 50 kW charger when operating interleaved is presented in figure 6.15. The harmonics surrounding the first switching frequency are suppressed as can be seen. The critical harmonic, at double the switching frequency, is at a sufficient level of 0.0014 times the fundamental. This has been accomplished with smaller filter components than compared with the normal operation case. The 266 μH inductor with a current rating of around 75 A has been replaced with two 133 μH inductors with only half the required current rating.

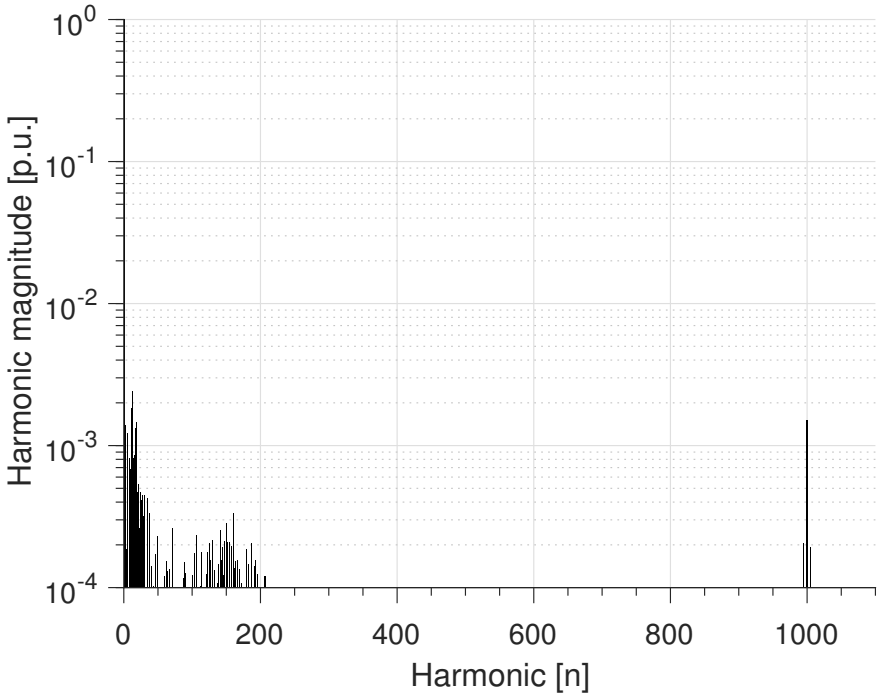

Figure 6.15: Harmonic content for currents drawn from grid (Simulation of 50 kW 25 kHz interleaved operation).

The numerical values are presented in table 6.4 for comparison. The low order harmonics are of similar magnitude, whereas the big difference is at the first switching frequency. The values satisfy the standard IEC 61000-3-4 which has a maximum limit of 0.6 % [32].

Table 6.4: Comparison of normal and interleaved operation of 50 kW charger.

Case	**Relative amplitude***		[%]
	f_{sw}	$2 \cdot f_{sw}$	THD
I1 normal operation	0.29	0.04	0.51
I1 interleaved operation	-	0.14	-

**Entries marked - are less than 10^{-4} times the fundamental.*

6.2.3 Simulated harmonic content for different grid impedances

Simulations are performed for the 50 kW charger when connected to different grid locations in order to get a sense of how it affects the current harmonics, but also the voltage harmonics. When a grid impedance is in-

troduced, the voltage at the PCC can vary, as opposed to when the voltage source was infinitely strong.

The impact that different grid impedance has on the harmonic results is shown in table 6.5. The observation that can be made is that the current harmonics are lower when the grid impedance rises, but the since the grid is weaker it is arguably also more sensitive to voltage harmonics, leaving them at a similar level for all grid impedances.

Table 6.5: Results for different grid impedances.

	Case		**Relative amplitude***		[%]
Entity	Charger	Grid no.	f_{sw}	$2 \cdot f_{sw}$	THD
I1	Siemens	#1	0.10	0.10	1.41
I1	50 kW	x	0.29	0.04	0.51
I1	50 kW	#1	0.02	-	0.70
I1	50 kW	#3	0.05	0.01	0.54
V1	Siemens	#1	0.13	0.27	0.17
V1	50 kW	#1	0.12	0.04	0.16
V1	50 kW	#3	0.11	0.03	-

**Entries marked - are less than* 10^{-4} *times the fundamental.*

6.3 Installation size and room for improvements

This section treats possibilities for reduced installation size with regards to the results from performed simulations and measurements. Some filter design parameters are discussed too.

As introduced in chapter 3.3.1 there is a large difference between allocated space and the utilised space in the installation on Lindholmen. Most of the allocated space is unused free space or *service space* and a very little portion is used by the converter and its transformer. However, measuring floor space the effective space for converter and transformer is approximately 2 m^2 (1 m^2 per unit, not including service space). If only the effective space of converter and transformer is considered and compared, the transformer uses approximately the same space as the converter. A high priority for reducing installation size would be to find alternatives to the transformer. One already suggested solution would be to replace the transformer with inductors and use a DC/DC converter on the secondary side of the converter for providing galvanic isolation, which would most likely reduce size. Another possible solution would be to connect the installation directly to the medium voltage grid through a 10/0.4 kV transformer instead. The

10/0.4 kV transformer could also serve as a grid side inductor and could provide galvanic isolation as well. Both solutions could have been effective for reducing installation size and rises opportunities for future research.

6.3.1 Filter size comparison of interleaved and normal operation

The resulting difference between the normal operation converter and paralleled interleaved converter is that there are two input inductors instead of one, and two full bridge converters. However, these two paralleled devices now only need a half the original current rating. In addition, the converter side inductor value has been halved, from one 266 μH inductor to two 133 μH inductors.

There are articles claiming that for specific types of inductors, if instead of using one, but two inductors, with reduced inductance and halved current rating the total size and weight is reduced [38]. From the numbers presented by [38], such an inductor substitution yields a rough 30 % size and weight reduction. This would mean that combined with in this thesis performed simulations of the interleaved operation, it can be concluded that a rough 30 % total size and weight reduction of the grid side inductor has been achieved. However, there are numerous types of inductor design parameters, different core materials, winding techniques, losses, and heat tolerance could all have different size dependencies on their ratings. To claim that the physical size of the new solution is reduced may not be true for all cases of inductors.

What also needs to be taken into account is that there is now two converter stages instead of one, although each with half the required current rating. The fact that two converter stages might require some extra space is evident but hopefully this is less than what is gained from the reduction of inductor size.

A conclusion that can be made from the work in this thesis is that the filter solution can be smaller and lighter when using interleaved operation. The simulations made has also shown that a converter with reduced inductor ratings still fulfilled the requirements on harmonic emissions.

6.3.2 Filter damping resistor losses

In section 4.3 the choice of damping resistors is discussed. Increasing the resistance implies lower resonance peak at the cost of increased losses. In the 50 kW model increasing the resistance value from 0.1 Ω to 1 Ω, increases losses in the resistors from 6.4 W to 52.8 W, almost ten times higher losses

when increasing resistance one order of magnitude. The internal series resistance R_{ESR} in a filter capacitor is typically a few $m\Omega$ and should be considered when selecting component. Compared to 50 kW, 6.4 W is only about 0.01 % and thus has a minor contribution to the overall efficiency of the converter. The choice of the lower resistance can further be motivated by that 50 W of heat-dissipation is undesirable not only for the efficiency. High heat-dissipation will lead to unnecessary large components and/or heat-sinks, in a closed cabinet it may also require increased ventilation. Selecting an appropriate value of this resistance is an important balance between losses and stability.

7

Discussion

This chapter contains discussions around the meaning of certain results as well as the trustworthiness of them. Some suggestions for future work is given as well.

7.1 Inability to localise sources of idle mode harmonics

As already introduced in chapter 6, the performed measurements on the operating Siemens charger showed signs of 3 kHz switching harmonics being present, even when the DC charging current and voltage was measured to zero. This suggests that switching at 3 kHz does occur even when there is no charging. Some sources of these measured harmonics seems more likely than others.

One, rather far fetched, alternative is that it comes from an external device, also utilising 3 kHz switching. This would in its turn be able to affect the voltage at the point where the Siemens charger is connected.

Another alternative, and the one we consider to be likely, is that the Siemens charger never stops switching and always maintains a certain dc voltage even though no charging occurs. The fact that no voltage or current was registered on the DC side during these moments could be explained by a breaker located on the DC link being disconnected. The breaker would have to be located closer to the converter than where the measurements were performed. The reason for never turning of the switching is unclear, since breakers could have been placed on the AC side of the converter. A suspicion can be that by leaving the converter and related electronic devices on, the amount of component failures, caused by for example frequent temperature fluctuations will be reduced.

Yet another source of harmonics could be other switched equipment fed trough the same transformer as the converter such as cooling fans, mechanic

control devices, or other electronics.

The impact at the constant switching harmonics seen in the measurement results has, is that the origin of some sources of harmonic contribution can not be located. If it was possible to turn off the charger and get clean values of idle voltages, the conclusion made on what harmonic contribution the charger has, would be more well founded. Let us reason on the possible options.

One of the rather clear observations made when looking at the harmonic content of the voltage is that there are switching harmonics present. Had we been able to turn off the charger station, we would have known if those were pre-existing and that there was some other switching device close by, or not. We have assumed that the 3 kHz components are from idle switching and show the full load harmonics without knowing if there is another device present.

The low order content of the idle voltage could have been concluded to be pre-existing in the grid, thus being able to tell how much low order harmonics the charger really contributed with. We can not know if fans, power electronic controls, or equipment connected to single phase power outlets, give rise to the low order harmonics.

As a suggestion for improvements or future work we would like to propose taking measurements again when the station is out of service to get the missing answers.

7.2 Higher grid impedance did not increase voltage harmonics

One of the more interesting results we have seen while running simulations is that for the 50 kW charger, changing the grid inductance did not change the resulting voltage harmonics to a large extent. The expected general behaviour was that a grid with higher short circuit impedance would be more sensitive to voltage drops. While that is obviously true, in the case of the grid connected LCL-filter of this size, the grid inductance actually contributed to the attenuation of the current well enough to keep the voltage harmonic levels at the switching frequency almost unchanged.

The requirement for this is that the extra grid impedance comes in the form of inductance. As long as the ratio between inductance and resistance is high enough, extra grid impedance should not affect the voltage too much. This, of course, depends on the filter type and on the parameters the switched device has. The side grid inductance of the LCL-filter is in this case 10 μH,

which in comparison with the largest given grid inductance of 124 μH, is not much.

With this in mind, can a filter solution be modelled to a bare minimum, just barely fulfilling the regulations and count on the extra impedance of the grid to take take off some extra desired margin? Certainly in the case of this thesis and the designed LCL-filter for the 50 kW application, even a strong grid connection did make a difference, lowering the current harmonics significantly. This is however a case where the grid side inductance is relative small, both compared to the converter side inductor and the inductance of the grid, suggesting it is sensitive to whatever is connected close to the converter.

No comparisons or tests have been made where the weighting of grid side inductance against converter side inductance is considered. Not only would it have been interesting to see what ratio between the two mentioned inductances yields the smallest solution for a specific attenuation. But also getting some numbers on what a minimum grid side inductor value should be for a certain charger rating in order to be able to operate and maintain the boost function. It is also interesting to know how sensitive the converter is to how robust the grid it is connected to, and a larger grid side inductance would perhaps be preferable to reduce those risks. As always, the controller design considerations and stability analysis has to take all of these matters into account. At least in the simulations performed as a part of this research, the addition of grid inductance has not caused any signs of stability problems.

7.3 The heavy vehicle chargers role in the urban environment

During the work of this thesis, there has been other projects within the subject of electric vehicles, its batteries and fast chargers. One of the more comprehensive goals have been to decrease size and/or weight with preserved performance. The bus chargers the authors have been in contact with during the thesis has been test-, evaluation- or pilot-projects. The converters have in common that they have been manufactured in small volumes, often with standard components not particularly designed for the purpose. This has resulted in installations taking up a great deal of space, perhaps more than it would have done if is was a well established product.

This can be seen as counteracting the incentives for these kinds of installations in a city environment. If batteries is to be a serious option for energy storage in vehicles for public transport, the size of the charging installation is of great concern if they are located in the city area. It is not obvious

that the size of the installation would decrease if the amount of installations increased but it is likely that an increased demand would imply more slimmed design and less bulky installations. The authors considers a smaller total installation size most necessary to achieve a high number of installations in an urban environment, where space is both expensive and in short supply.

In the case with the Siemens installation a transformer, which also likely serves as a grid side inductor of an LCL-filter, is installed towards the grid to provide galvanic isolation. This three phase transformer is taking up a great part of the utilised space in the installations and if the function and protection this device supplies could be achieved in another way, the size could be decreased considerably. These installations have all been located indoors, in a dedicated building or located in an already existing building where plenty of space is left for service. If the need of service space could be excluded the whole installation could be considerable smaller. If the installation could be made smaller and located in a smaller housing for example at the side of a pavement, a technician could use space of the pavement as service space during service visits.

The authors agree that it is of high importance to decrease the converter and filter size to facilitate installations in city environments. It is however important to keep a holistic view of the total installation size and try to reduce where large changes can be done with small effort so one does not spend resources on making a converter smaller only to put it in an unnecessarily large casing.

7.4 Measurement results vs regulations

There are differences between the mentioned standards in the section about grid codes. For example within the subject of THD, the Swedish regulations, IEEE and IEC is counting a different number of harmonics. They have however one thing in common, they are all far away from covering harmonics around the switching frequencies in question. To state what consequences harmonics at these frequencies give, a deeper examination is needed. But one can speculate about if the standards should have more detailed demands on higher orders of harmonics.

Will we see lower demands on voltage stability as large synchronous machines become fewer. With wind and solar expanding there is a debate regarding why we need a stable frequency with low harmonic content. Maybe as the, in for example Sweden right now, nuclear is dismantled and the number of machines that demand stable 50 Hz grid frequency is reduced. Is it possible that we at some point will reach a, with today's standards, poor power quality on the transmission/distribution grid? The customers

that do have high demands on power quality will have to take care of that themselves with custom power devices.

7.5 Lack of prototype

As so often when dealing with scientific research, the results giving the most reliability are those from real physical tests, on actual electronics. Many things risk to get overlooked when only using simulation results as a foundation for the research. This gets particularly important when reaching higher switching frequencies, such as with the 25 kHz of this thesis. For example inductances and capacitances are frequency dependant and care should be taken when realising a high frequency switching device because of problems that arise because of this. Stray capacitances, simplifications in switching patterns and other non idealities for components are also examples of sources for errors. There is a risk that simplifications that were necessary for calculations and simulations can cause unexpected results when a prototype is to be built. Naturally it would have been desirable to build a prototype to test an verify adequate results presented earlier in this thesis. Now this opens opportunities for future work and research.

7.6 Interleaving - challenges and possibilities

The idea with a converter operating interleaved with two switching stages showed very good results in the simulations and, with good design, can also provide for some redundancy if one stage fails. I.e. a converter has two stages and normally operates interleaved, if one of the converter stages fails the remaining stage may continue to operate and the converter would be able to supply half of its original power. During this redundancy operation mode the converter will however not enjoy the benefit of cancellation of the first switching harmonic, and a designer is recommended to take this in consideration during a design procedure. There are many benefits of interleaved operation but the concept contributes with both increased functionality and complexity to the converter, which in the long run risks decreasing reliability.

7.7 The need for electrification of vehicles

We need electric vehicles, at least that is what we think - But comes with a few conditions. Electrification of vehicles and the support for charging them is just in its early years. The automotive industry has had almost a hundred years to perfect the combustion engine and its applications. Already the electric vehicles are up there matching the performance in many considerations. Imagine where the electric car stands after decades more of perfection. However, the main argument for electrification is in our view not the possibilities for extra performance. The main argument is the possibilities for a sustainable form of transportation. Sure, the electric car is not perfect in that regard. It still struggles with rare earth materials being mined under poor conditions in third world countries and the battery has been a headache for some time. An important thing to point out is that the means of making it clean are already here. Sustainable electric energy is out there for harvesting, through e.g. wind and solar, but society still relies on burning fossil fuels for electric energy to a large extent. At least the electric car has possibilities we look for, that the combustion engine car does not have. It will not exhaust particles and contribute to smog in urban areas, a problem already affecting Swedish cities which are not even considered large in the global perspective. It will, less than a combustion engine vehicle, contribute to noisy environment, harmful for both people and nature. Most importantly, the electric vehicle can be driven on pure energy. A general opinion is that society is suffering from an energy crisis but the solutions are already there. The societal responsibility is now to urge on a sustainable development of electric vehicles as well as we can. We should urge the development of environmentally sustainable sources because with the electric power generation of today it will in many cases not help. We need electric vehicles, but we need them in the correct manner.

8

Conclusion

It has, through performed measurements and investigation of grid regulations, been shown that the existing charger installation fulfils found regulations on voltage quality.

A proposed design of a 50 kW charger has been tested with different grid conditions. Simulations has shown that the grid inductance did not cause instability or resonance issues in the performed experiments but rather increases the damping. It can be concluded that in performed research, the filter design could be made using minimum margin, considering no grid impedance, and in the real application the connecting grid will provide extra attenuation to give some margin for poor component accuracy etc.

By combining already existing literature and performed simulations it has been shown that there are good opportunities for size reduction by using interleaved operation.

References

[1] T. Maxian Rusche, "The european climate change program: An evaluation of stakeholder involvement and policy achievements", English, *Energy Policy*, vol. 38, no. 10, pp. 6349–6359, 2010, ISSN: 0301-4215.

[2] T. Thiringer, "Power quality evaluation of the opbrid charger station", Chalmers University of Technology, Tech. Rep., 2013.

[3] M. Liserre, F. Blaabjerg, and S. Hansen, "Design and control of an lcl-filter-based three-phase active rectifier", *IEEE Transactions on Industry Applications*, vol. 41, no. 5, pp. 1281–1291, Sep. 2005, ISSN: 0093-9994.

[4] M. A. Ahmed, J. D. Dasika, M. Saeedifard, and O. Wasynczuk, "Interleaved swiss rectifiers for fast ev/phev battery chargers", in *2014 IEEE Applied Power Electronics Conference and Exposition - APEC 2014*, Mar. 2014, pp. 3260–3265.

[5] J. R. Rodriguez, J. W. Dixon, J. R. Espinoza, J. Pontt, and P. Lezana, "PWM regenerative rectifiers: State of the art", *IEEE Transactions on Industrial Electronics*, vol. 52, no. 1, pp. 5–22, Feb. 2005, ISSN: 0278-0046.

[6] A. Reznik, M. G. Simões, A. Al-Durra, and S. M. Muyeen, "LCL filter design and performance analysis for grid-interconnected systems", *IEEE Transactions on Industry Applications*, vol. 50, no. 2, pp. 1225–1232, Mar. 2014, ISSN: 0093-9994.

[7] S. Jayalath and M. Hanif, "Generalized LCL-filter design algorithm for grid-connected voltage-source inverter", *IEEE Transactions on Industrial Electronics*, vol. 64, no. 3, pp. 1905–1915, Mar. 2017, ISSN: 0278-0046.

[8] M. A. Mosa, A. A. Elsyed, A. M. A. Amin, and A. M. A. Ghany, "Modified design of an LCL-filter for grid-connected, pulse-width-modulated voltage source converter", in *2016 Eighteenth International Middle East Power Systems Conference (MEPCON)*, Dec. 2016, pp. 89–94.

[9] Z. Wu, M. Aldeen, and S. Saha, "A novel optimisation method for the design of LCL-filters for three-phase grid-tied inverters", in *2016 IEEE Innovative Smart Grid Technologies - Asia (ISGT-Asia)*, Nov. 2016, pp. 214–220.

[10] K. Xing, F. C. Lee, D. Borojevic, Z. Ye, and S. Mazumder, "Interleaved pwm with discontinuous space-vector modulation", *IEEE Transactions on Power Electronics*, vol. 14, no. 5, pp. 906–917, Sep. 1999, ISSN: 0885-8993.

[11] D. Shin, J. P. Lee, T. J. Kim, D. W. Yoo, and H. J. Kim, "Comparative evaluation of coupling L-CL filter for interleaved three-phase voltage source inverters", in *2015 9th International Conference on Power Electronics and ECCE Asia (ICPE-ECCE Asia)*, Jun. 2015, pp. 2388–2394.

[12] S. M. Sharkh, M. A. Abu-Sara, G. I. Orfanoudakis, and B. Hussain, "Design and control of a grid-connected interleaved inverter", in *Power Electronic Converters for Microgrids*. Wiley-IEEE Press, 2014, pp. 352–, ISBN: 9780470824054.

[13] A. V. Oppenheim and A. S. Willsky, *Signals and systems*, 2nd ed. New Jersey: Prentice-Hall International, Inc, 1997, ISBN: 0-13-651175-9.

[14] D. Shmilovitz, "On the definition of total harmonic distortion and its effect on measurement interpretation", *IEEE Transactions on Power Delivery*, vol. 20, no. 1, pp. 526–528, Jan. 2005, ISSN: 0885-8977.

[15] "Spänningens egenskaper i elnät för allmän distribution", *SVENSK STANDARD SS-EN 50160*, Dec. 2011.

[16] "IEEE recommended practice and requirements for harmonic control in electric power systems", *IEEE Std 519-2014 (Revision of IEEE Std 519-1992)*, pp. 1–29, Jun. 2014.

[17] N. Mohan, T. M. Undeland, and W. P. Robbins, *Power electronics*, 3rd ed. John Wiley & Sons, Inc., 2003, ISBN: 0-471-42908-2.

[18] D. G. Holmes and T. A. Lipo, "Zero space vector placement modulation strategies", in *Pulse Width Modulation for Power Converters:Principles and Practice*. Wiley-IEEE Press, 2003, pp. 259–336, ISBN: 0-471-20814-0.

[19] C. Chang and M. A. Knights, "Interleaving technique in distributed power conversion systems", *IEEE Transactions on Circuits and Systems I: Fundamental Theory and Applications*, vol. 42, no. 5, pp. 245–251, May 1995, ISSN: 1057-7122.

[20] F. Forest, E. LabourÉ, T. A. Meynard, and V. Smet, "Design and comparison of inductors and intercell transformers for filtering of pwm inverter output", *IEEE Transactions on Power Electronics*, vol. 24, no. 3, pp. 812–821, Mar. 2009, ISSN: 0885-8993.

[21] J. C. Das, "Passive filters", in *Power System Harmonics and Passive Filter Designs*. Wiley-IEEE Press, 2015, pp. 685–744, ISBN: 9781118887059.

[22] S. Seo, Y. Cho, and K.-B. Lee, "LCL-filter design for grid-connected three-phase inverter using space vector PWM", English, IEEE, 2016, pp. 389–394.

[23] M. J. Nave, *Power line filter design for switched-mode power supplies*. New York: Van Nostrand, 1991, ISBN: 0-442-00453-2.

[24] J. C. Das, "Passive filters", in *Power System Harmonics and Passive Filter Designs*. Wiley-IEEE Press, 2015, pp. 427–452, ISBN: 9781118887059.

[25] "Electromagnetic compatibility (EMC) - part 3-6: Limits - assessment of emission limits for the connection of distorting installations to MV, HV and EHV power systems", *IEC/TR 61000-3-6*, pp. 1–58, Feb. 2008.

[26] "Energimarknadsinspektionens föreskrifter och allmänna råd om krav som ska vara uppfyllda för att överföringen av el ska vara av god kvalitet", *EIFS 2013:1*, Aug. 2013, ISSN: 2000-592X.

[27] S. M. Halpin, "Comparison of IEEE and IEC harmonic standards", in *IEEE Power Engineering Society General Meeting, 2005*, Jun. 2005, 2214–2216 Vol. 3.

[28] "IEEE recommended practices and requirements for harmonic control in electrical power systems", *IEEE Std 519-1992*, pp. 1–112, Apr. 1993.

[29] ElectriCity. (Feb. 2017). Elbussen – tyst, avgasfri och passagerarvänlig, [Online]. Available: `http://www.goteborgelectricity.se/node/19499/om-elbussen`.

[30] OppCharge. (May 2017). This is oppcharge, [Online]. Available: `https://www.oppcharge.org/dok/This_is_OppCharge.pdf`.

[31] S. Haghbin, A. Rabiei, and T. Thiringer, "High-frequency modelling of a three-phase pulse width modulation inverter towards the dc bus considering line and controller harmonics", *The Journal of Engineering*, Jan. 2014, ISSN: 2051-3305.

[32] "Electromagnetic compatibility (EMC) - part 3-4: Limits - limitation of emission of harmonic currents in low-voltage power supply systems for equipment with rated current greater than 16 A", *IEC/TS 61000-3-4*, pp. 1–29, Oct. 1998.

[33] J. C. Das, *Power system harmonics and passive filter designs*. Wiley-IEEE Press, 2015, ISBN: 978-1-11-888705-9.

[34] V. H. Prasad, "Analysis and comparison of space vector modulation schemes for three-leg and four-leg voltage source inverters", Master's thesis, Virginia Polytechnic Institute and State University, 1997.

[35] D. G. Holmes and T. A. Lipo, *Pulse width modulation for power converters:principles and practice*. Wiley-IEEE Press, 2003, ISBN: 0-471-20814-0.

[36] R. Ottersten, "On control of back-to-back converters and sensorless induction machine drives", PhD thesis, Chalmers University of Technology, 2003, ISBN: 91-7291-296-0.

[37] P. C. Buddingh, "Even harmonic resonance-an unusual problem", *IEEE Transactions on Industry Applications*, vol. 39, no. 4, pp. 1181–1186, Jul. 2003, ISSN: 0093-9994.

[38] L. Asiminoaei, E. Aeloiza, P. N. Enjeti, and F. Blaabjerg, "Shunt active-power-filter topology based on parallel interleaved inverters", *IEEE Transactions on Industrial Electronics*, vol. 55, no. 3, pp. 1175–1189, Mar. 2008, ISSN: 0278-0046.

A

Appendix

Voltage controller

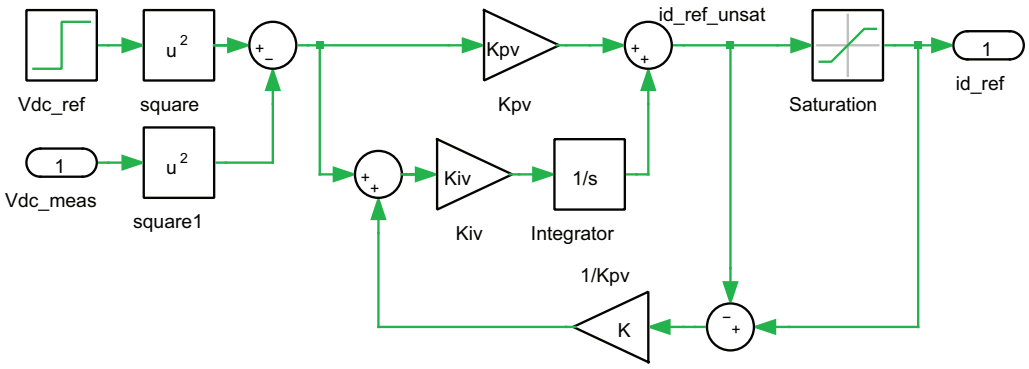

Figure A.1: Voltage controller. Features anti windup.

Current controller

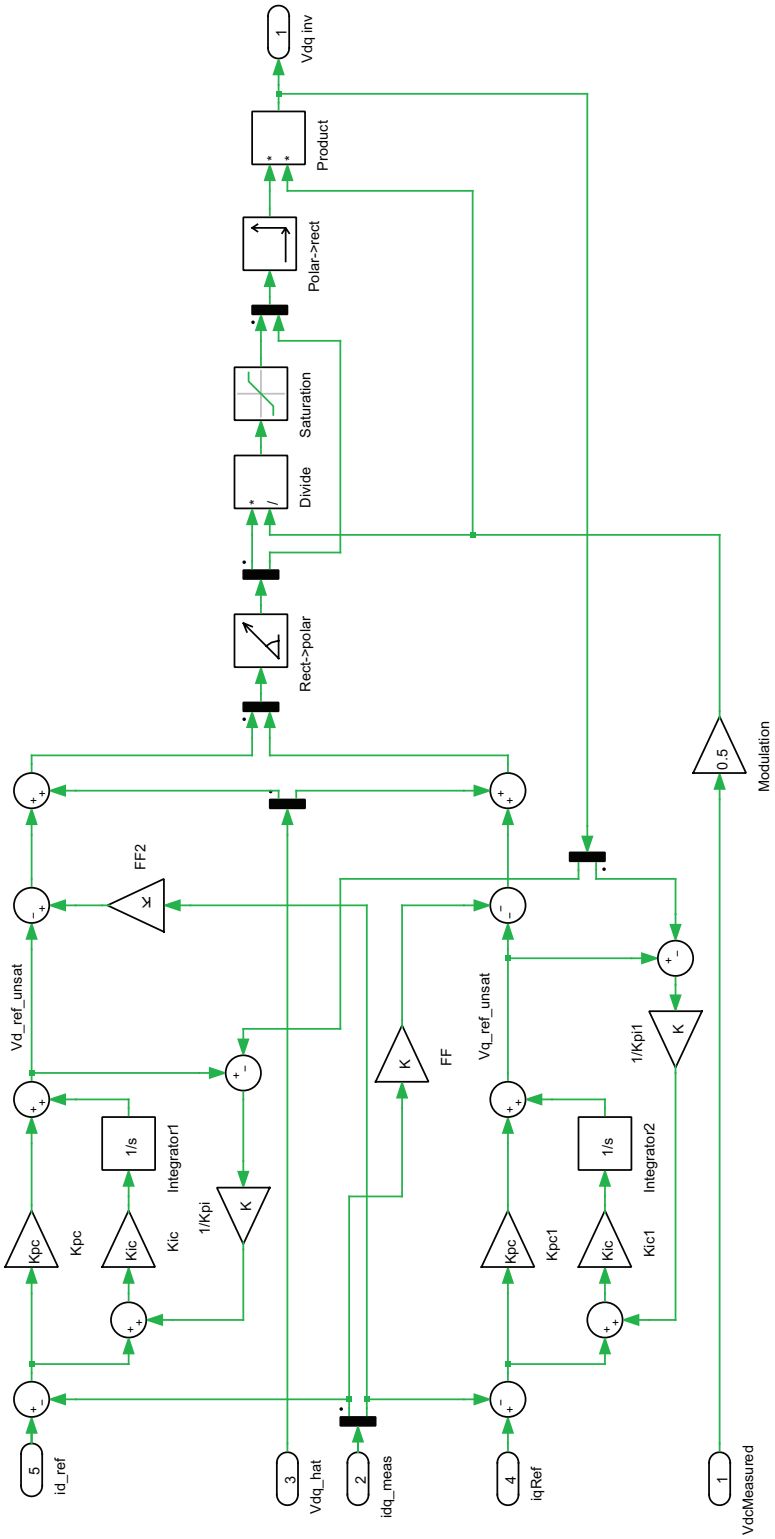

Figure A.2: Current controller. Features anti windup, cross coupling and feed forward.